Sexual reproduction is controlled by successive transcriptomic waves in *Podospora anserina*

Frédérique Bidard[1, 2, §], Pierre Grognet[3, §], Gaëlle Lelandais[3, §], Sandrine Imbeaud[4, 5], Marie-Hélène Mucchielli[4, 6], Robert Debuchy[1, 3], Véronique Berteaux-Lecellier[1, 7, #] and Fabienne Malagnac[3, #, *].

[1] Univ Paris-Sud 11, CNRS, Institut de Génétique et Microbiologie UMR8621, F- 91405 Orsay, France.

[2] IFP Energies Nouvelles, 1 et 4 avenue de Bois-Préau, 92852Rueil-Malmaison, France

[3] Université Paris-Saclay, CEA, CNRS, Institute for Integrative Biology of the Cell (I2BC), 91198, Gif-sur-Yvette, France

[4] CNRS, Centre de Génétique Moléculaire, FRE3144, GODMAP, 91190 Gif sur Yvette, France.

[5] present address : INSERM, Génomique Fonctionnelle des tumeurs solides, UMR U-674, IUH, Université Paris Descartes, 75010 Paris, France.

[6] present address : Institut de Sciences des Plantes - Paris-Saclay, Bâtiment 630, Avenue des Sciences, 91190 Gif-sur-Yvette, France

[7]present address: CNRS, IRD, Univ. Nouvelle Calédonie, Univ. La Réunion, EMR9001 SANTECO, ENTROPIE, Nouméa, New Caledonia

[§] **Contributed equally**

[#] **Contributed equally**

[*]**Corresponding author**

Correspondence: fabienne.malagnac@universite-paris-saclay.fr

Abstract

Despite the inherent challenge of finding suitable mating partners, most eukaryotes use sexual reproduction to produce offspring endowed with increase genetic diversity and fitness. The persistence of this mode of reproduction is a key question in evolutionary biology. Fungi offer valuable insights into this question, due to their diversity and short lifecycle. This study focuses on *Podospora anserina*, a pseudohomothallic ascomycete fungus that bypasses self-sterility by maintaining two compatible nuclei in one mycelium. We performed genome-wide gene expression profiling during ten stages of *P. anserina* sexual reproduction and identified five major expression patterns. Our expert annotation approaches identified differentially expressed genes related to secondary metabolite production, fungal vegetative incompatibility, programmed cell death, and epigenetic regulation. In addition, master transcriptional regulators and their target networks were uncovered. This study provides a comprehensive database for future functional genomics experiments and novel pathway characterization during sexual reproduction.

Keywords: transcriptome, time-course, sexual differentiation, filamentous fungi

Running head: Transcriptome landscape during fungal sexual development

Introduction

Most eukaryotes rely on sexual reproduction to produce offspring. However, the maintenance of sex remains a fundamental question in evolutionary biology. The amazing diversity of fungi makes them of particular interest for addressing this question. Fungi are found in almost every terrestrial and marine ecosystems (Stajich *et al*. 2009; Breyer and Baltar 2023). Some play key roles in biogeochemical cycles, while others possess traits that enable them to be pathogenic to plants or animals (Iliev *et al*. 2024). Understanding the biology of fungi, and in particular why many of them can produce either asexual or meiotic products depending on environmental conditions (Dyer and Kück 2017; Wang *et al*. 2018), is crucial for fields as diverse as ecology, agronomy and human health.

For fungi, as for all eukaryotes, sexual reproduction has well-documented advantages. In particular, meiosis, the sex-specific division, reduces the accumulation of deleterious mutations and can link beneficial alleles that are subsequently fixed in populations by natural selection (Otto 2009). In harsh environments, sexual reproduction, as opposed to asexual reproduction, can lead to improved fitness of the offspring.

Fungal sexual reproduction relies on a wide range of developmental strategies and mating systems. These include both inbreeding, in which a single individual can self-fertilize, and obligate outbreeding, in which only genetically distinct compatible partners can mate. Some fungi, referred to as pseudohomothallic, have managed to retain the best of each strategy. Pseudohomothallism extends the diversity of reproductive systems evolved in fungi by selecting breeding systems that allow self-sterility to be bypassed by maintaining two populations of compatible nuclei in the same mycelium (Peraza-Reyes and Malagnac 2016). Early forward genetic screens and more recent transcriptomic studies in Sordariomycetes (Wang *et al*. 2014; Lütkenhaus *et al*. 2019; Kim *et al*. 2022) have led to the identification of large sets of genes involved in specialized developmental pathways that control the fertilization and the subsequent developmental stages (Wilson *et al*. 2019). Some of these species were heterothallic (self-incompatible, self-sterile (Wang *et al*. 2014; Lütkenhaus *et al*. 2019)), while others were homothallic (self-compatible, self-fertile (Teichert *et al*. 2012; Wang *et al*. 2019)). However, how the development of meiotic tissues within the fruiting body is controlled and which genes are critical in this process remains unknown.

In this study, we propose to approach this question from a different angle using the pseudohomothallic species *Podospora anserina*. This species is used as a model system for the study of the fruiting body development (Peraza-Reyes and Malagnac 2016) but a detailed

analysis of the cellular programs allowing its formation from fertilization to ascospore discharge was lacking. In this context, we performed a genome-wide gene expression profiling during the sexual reproduction of *P. anserina* at ten time points representing key developmental steps. To characterize the topology of differential gene expression profiles across sexual reproduction, we analyzed our transcriptomic data using two complementary approaches: *i)* a data-driven approach using k-means clustering and *ii)* a biological expertise-driven approach to mine the gene functions. The data-driven approach revealed five major patterns (waves) of differential expression during sexual development. The expert annotation approach has led to the identification of a number of interesting gene categories, including secondary metabolites and toxins encoding genes, genes responsible for fungal vegetative incompatibility programmed cell death, and gene related to epigenetic effectors that interfere with messenger stability (RNAi/MSUD genes. Finally, we identified several master transcriptional regulators and draw their potential target gene network. Overall, our study has produced a comprehensive database that offers numerous candidates for functional genomics experiments. This database also paves the way for the characterization of new pathways during sexual reproduction.

96 # Materials and methods

97 ## *Podospora anserina* strains and methods

98 *P. anserina* is a filamentous ascomycete whose life cycle and general methods have
99 already been described (Esser 1974; Rizet and Engelmann, 1949; Zickler *et al*., 1995). All
100 strains used in this study were derived from the *S* strain (Rizet and Engelmann 1949; Espagne
101 *et al*. 2008). Growth and crosses of *S mat*+ and *S mat*- strains were carried out on a minimal
102 synthetic medium (M2 medium) at 27°C with constant light (Silar 2020). The *136* strain is
103 described in (Coppin and Silar 2007).

104 ## Cytology

105 Sexual cells were either fixed in 7.4% paraformaldehyde and processed for microscopy
106 as previously described (Thompson-Coffe and Zickler, 1994) or directly observed in M2
107 medium. When required, nuclei were stained with DAPI (4',6-diamidino-2-phenylindole, 1
108 mg/mL; Boehringer Ingelheim). Observations were performed with a Zeiss Axioplan
109 microscope, and images captured with a CDD Princeton camera system.

110 ## Time-course procedure and RNA isolation

111 To facilitate biological materials collecting, we used cellophane sheets (cat # 1650193,
112 Bio Rad Laboratories, Hercules) and cheesecloth pieces (Nitex 03-48/31, Sefar AG, Heiden),
113 which were deposited on M2 medium prior to inoculation. Cellophane sheets avoid the
114 contamination of biological material by M2 medium when scraping mycelium. The mesh of
115 cheesecloth accommodates the mycelium, while perithecia develops above the mesh and can
116 be scraped with minimal mycelium contamination. S mat- strain has been used as male gamete
117 donor and *S mat*+ strain as female. The *S mat*+ strain was grown on cellophane sheet for the
118 analysis of mycelium and on cheesecloth for analysis of perithecial development. The
119 biological material was then collected 6, 12, 18, 24, 30, 42, 54 and 96 hours after fertilization
120 and an additional time point 24 hours prior fertilization was taken. Three biological replicates
121 issued from three independent time course have been collected for all time points and two for
122 T42, as we discarded the third and the back-up replicates, which did not meet our quality
123 requirements.

124 For each ten points of the time course, the number of Petri dishes has been adjusted (five
125 were used for T-24h, T0h, T6h, T18h, T24h, four for T30h, two for T42h, one for T54h and
126 T96h) to collect 20 to 100 mg of fertilization competent mycelium or/and perithecia. One to

127 five Petri dishes *per* time course experiment were thus inoculated simultaneously with a
128 growing *S mat-* strain and spermatia were collected by washing with 1.5 ml of H_2O six days
129 later. The collected spermatia (around 10^4 spermatia per ml) were pooled and then used to
130 fertilize a corresponding number of Petri dishes of 4-day-old *S mat+* strain. The moment just
131 prior the fertilization process was considered as the T0 (0 hours).

132 The biological material collected by scraping gently either cellophane or cheesecloth
133 with a cover glass, was dried out with filter paper, weighted, frozen in liquid nitrogen and stored
134 at -80°C. Total RNAs of *P. anserina* were extracted using RNeasy Plant Mini Kit (Qiagen),
135 including a grinding process using a Mikro-Dismembrator (Sartorius) and a DNase treatment.
136 The quality and quantity of the total RNAs was determined by using a Nanodrop
137 spectrophotometer (Nanodrop Technologies) and the Bioanalyzer 2100 system (Agilent
138 Technologies) as previously described in (Imbeaud *et al*. 2005).

139 **Gene expression array-based hybridization**

140 Transcriptome microarray experimental procedure, *i.e.* targets preparation,
141 hybridization and washing, was done following the two-color microarray-based gene
142 expression analysis instructions (version 5.0, February 2007) as described by the manufacturer
143 (Agilent Technologies). One-µg aliquots of total RNA were labelled using the Low RNA input
144 fluorescent linear amplification (LRILAK) PLUS kit (Agilent Technologies); internal standards
145 came from the Two-color RNA spike kit (Agilent technologies). The labelling efficiency and
146 the product integrity were checked as described by (Graudens *et al*., 2006). The reference cRNA
147 was labelled with Cy5 and sample probes with Cy3. Briefly, the reference RNA pool was
148 prepared by mixing equal amounts of RNA extracted from mycelium at 48 h and 96 h post-
149 inoculation, and from perithecia at 24 h, 48 h and 96 h post-fertilization (Bidard *et al*. 2010).
150 This composition allows a detectable and stable expression signal on the majority of CDS
151 (Bidard *et al*. 2010). Then, Cy3- and Cy5-labeled targets were mixed and incubated on an
152 Agilent microarray slide for 17 hours at 65°C, in a rotating oven (6 rpm for a 1x44K and 10
153 rpm for a 4x44K array format), using an Agilent *in situ* hybridization kit. The slides were
154 washed and then any traces of water were removed by centrifugation at 800 rpm for 1 min
155 (Bidard *et al*. 2010; Bidard *et al*. 2011).

156 **Data acquisition from microarray experiments**

157 Microarrays were scanned using an Agilent dual laser DNA microarray scanner (Agilent
158 Technologies), model G2567AA, with 5-µm resolution. The resulting 16-bit image files were

159 analyzed in the *Feature Extraction* processing system (FE, v9.5.3). Spot and background
160 intensities were extracted and normalized with the Feature Extraction software using the GE2-
161 v4_95_Feb07 default protocol (Local background subtracted and LOWESS normalization).
162 Preliminary array quality was assessed using Agilent control features as well as spike-in
163 controls (Agilent 2-Color Spike-in Kit for RNA experiment). Subsequent flagging was done
164 according to the GenePix Pro software (Molecular Devices Syunnyvale, CA, USA)
165 nomenclature, including four levels of flags (good (100), bad (-100), not found (-50), moderate
166 (0)) and raw data normalization was performed as previously described in articles such as
167 (Bidard *et al*. 2010; Bidard *et al*. 2011). Briefly, it consisted in using standard bioinformatics
168 protocols to first filter probes with good quality flags, then correct signal intensities considering
169 global and local background noises, and finally correct for systematic bias between Cy3 and
170 Cy5 signals.

171 **Graphical summary of data analysis**

172 A schematic representation of the obtained data set is shown in Supplementary Figure
173 1 (see number #1). Gene expression measurements were thus analyzed according to two
174 different strategies, allowing to study either the co-expression between any pairs of annotated
175 genes in the *P. anserina* genome (see number #2) or the differential expression for all annotated
176 genes in the *P. anserina* genome between any pairs of time points (see number #3). For this,
177 gene expression profiles were calculated and statistical analyses to search for differentially
178 expressed genes were performed (see the following sections for more details).

179 **Calculation of gene expression profiles**

180 For each gene, "A values" were computed at each time point and for each replicate, with
181 the following formula: $A_{g,t,r} = \frac{1}{2}\left(log_2\left(G_{g,t,r}\right) + log_2\left(R_{g,ref}\right)\right)$, where $G_{g,t,r}$ represents the
182 normalized Cy3 intensity value measured for gene g at time point t in biological replicate r,
183 and $R_{g,ref}$ represents the normalized Cy5 intensity value measured for gene g in the reference
184 RNA pool (see previous sections). At each time point, triplicated values were next averaged to
185 obtain one value per time point, noted $A_{g,t}$. The mean and the median values, respectively noted
186 A_{mean} and M_g, and associated with $A_{g,t}$ values over all time points, were finally calculated and
187 used to adjust expression measurements for each gene around a new median value of 0, *i.e.*
188 $A^*_{g,t} = A_{g,t} - M_g$. An expression profile for a gene g is therefore made with ten A^* values which
189 are: $A^*_{g,Tm24}$; $A^*_{g,T0}$; $A^*_{g,T6}$; $A^*_{g,T12}$; $A^*_{g,T18}$; $A^*_{g,T24}$; $A^*_{g,T30}$; $A^*_{g,T42}$; $A^*_{g,T54}$; $A^*_{g,T96}$. Notably, it
190 represents the expression fluctuations of the gene over the time course.

191 **Statistical analyses to search for differentially expressed genes**

192 Gene expression measurements between pairwise time points were compared using the
193 MAANOVA (MicroArray ANalysis Of Variance) package (version 1.14.0) (Wu *et al*., 2003).
194 It allows fitting an ANOVA model as proposed by (Kerr and Churchill 2001) and provides a
195 way to consider multiple sources of variation in the microarray experiments. P-values were
196 computed by permutation analysis and were adjusted by the false discovery rate step-up method
197 of Benjamini and Hochberg to account for multiple testing (Benjamini and Hochberg, 1995).
198 From all comparisons, lists of differentially expressed genes (Table S1) were defined using
199 several filtering strategies:

200 - Filter #1 to select the genes with *(i)* an adjusted p-value < 0.05, *(ii)* a fold change ≥ 4 or
201 ≤ -4 with a A_{mean} ≥ 4.5,

202 - Filter #2 to select the genes with *(i)* an adjusted p-value < 0.001 and *(ii)* a fold change
203 ≥ 2 or ≤ -2 (*i.e.* absolute value of log2(fold change) ≥1).

204 The two lists of genes were used respectively for unsupervised clustering (see below) and
205 biological interpretations (see the Results section).

206 **PCA analysis and unsupervised clustering based on gene expression profiles**

207 Expression profiles of all genes were used for principal component analysis using the
208 function "pca" available in the R package mixOmics (Table S2) and expression profiles of
209 differentially expressed genes (selected based on Filter #1, see previous section) were used for
210 cluster analyses. To this list, the expression profiles of genes coding for mating-type
211 transcription factor SMR1, SMR2 and FMR1 were added. A hierarchical clustering (UPGMA
212 method) and several K-means clustering were computed independently using Spotfire
213 DecisionSite software package (Spotfire, Somerville, Mass.) with correlation coefficient as
214 similarity measure between A^* values in gene expression profiles. Intersection of clusters
215 obtained by the two-clustering method results in robust clusters (Table S1) from which the
216 temporal waves (see Result section) were derived.

217 **Sequence comparisons to search for orthologous genes with other species**

218 Orthologous genes were searched between *P. anserina* and the other species
219 *Neurospora crassa*, *Sordaria macrospora*, *Chaetomium globosom* and *Trichoderma reesei*. For
220 this purpose, protein sequences were downloaded from Uniprot (https://www.uniprot.org/)
221 under the accession numbers: UP000001805_367110 (*N. crassa*), UP000001881_771870 (*S.*

222 *macrospora*), UP000001056_306901 (*C. globosum*) and UP000008984_431241 (*T. reesei*).
223 The OrthoFinder algorithm (Emms and Kelly 2019) was used with default parameters to obtain
224 "orthogroups" (Table S3), *i.e.* groups of genes that are good candidates to share a common
225 ancestor between the compared species.

226 **Functional enrichment of terms associated with lists of genes**

227 Gene Ontology (Ashburner *et al*. 2000; The Gene Ontology Consortium *et al*. 2023) and
228 Pfam annotations (Mistry *et al*. 2021) were used to explore the biological relevance of the lists
229 of genes that composed the temporal waves (Table S4 and S5). P-values were calculated using
230 Fisher's exact test and following the methodology described in (Boyle *et al*. 2004).

231 **Expert annotation of *P. anserina* genes**

232 Expert annotation (Table S6) was performed using either BLASTP reciprocal best-hit
233 and/or Pfam conserved motif analyses. Output results were all validated after careful manual
234 inspection including the use of the FungiBD database for orthologs verifications (Basenko *et*
235 *al*. 2018).

236 **Co-expression network based on expression profiles of genes coding for transcription**
237 **factors**

238 Expression profiles of differentially expressed genes (selected based on Filter #2, see
239 previous section) for which the expert annotation was associated with "transcription factors"
240 (Table S7) were used to search for significant correlation (> 0.95) with the expression profiles
241 of all genes previously classified into transcriptional waves. Selected gene pairs were used to
242 represent a co-expression network as defined in (Wolfe, Kohane, and Butte 2005), in which all
243 potential links of transcriptional control, between the TF and another gene (referred to as "target
244 gene") are shown.

245 **Availability of data and source code, website to explore the results**

246 The raw data have been deposited in the MIAME compliant Gene Expression Omnibus
247 database (Edgar, Domrachev, and Lash 2002) and is accessible through the GEO Series
248 accession number GSE21659
249 https://www.ncbi.nlm.nih.gov/geo/query/acc.cgi?acc=GSE93094. The source code has been
250 deposited at : https://github.com/Podospora-anserina/transcriptome_kinetics_development/).
251 To explore the results for a particular gene or for a set of genes, we have created a WEB
252 application which is available at: https://pierregrognet.shinyapps.io/cinetique_app/.

253 # Results

254 ## High-resolution kinetics of transcriptional fluctuations during sexual reproduction

255 To ensure an accurate, high-density representation of transcriptional variation, we
256 collected RNA samples at ten key time points during the sexual reproductive cycle of *P.*
257 *anserina* (Fig. 1).

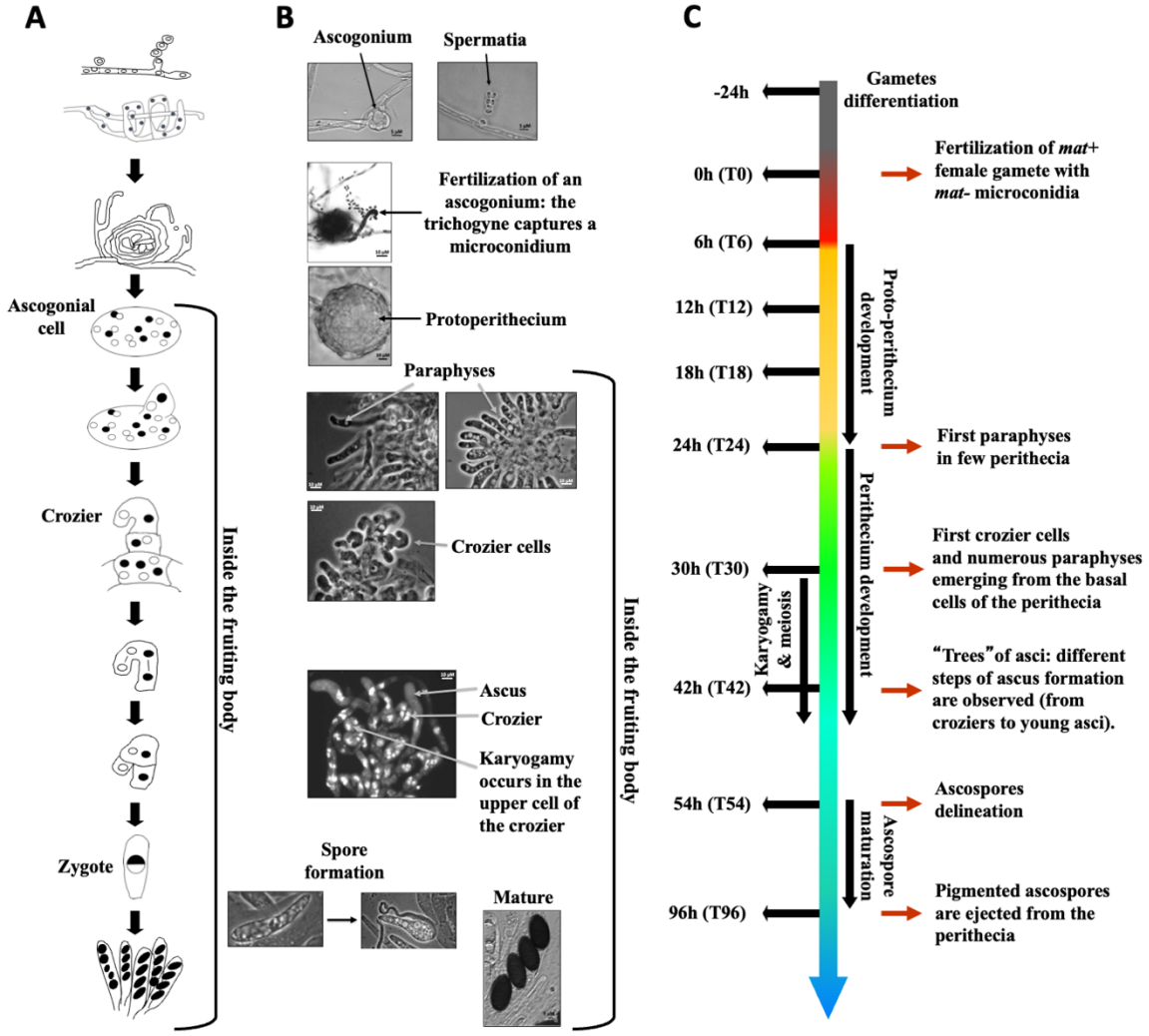

258
259

260 **Figure 1 - *P. anserina* developmental time course from fertilization to ascospore**
261 **maturation. A.** Schematic representation of the fertilization and the main steps of
262 zygotic development. **B.** Pictures of the main steps of sexual development. Sexual
263 reproduction began with the production of male (spermatium) and female
264 (ascogonium) gametes. A pheromone/receptor signaling system allows the female
265 gametes to attract specialized hyphae (trichogynes) that recognize and fuse with male
266 gametes of compatible mating type. This event initiates the multi-step process of
267 sexual development that begins with the formation of fructifications and ends with

268 the discharge of ascospores. The nucleus of the male gamete enters the trichogyne,
269 migrates along this specialized hypha, reaches the ascogonium and undergoes
270 several mitotic divisions. Fertilization (T0) triggers the development of
271 protoperithecia (T6 to T24), which recruit multiple layers of protective maternal
272 hyphae to grow into perithecia (T24 to T45). The developing fructifications shelter
273 the fertilized ascogonial cells (T24 to T30), which contain multiple haploid parental
274 nuclei of either *mat*+ or *mat*- genotype. Differentiation of paraphyses begins (T24)
275 just before three-celled hook-shaped structures called croziers emerge from the
276 ascogonial cells (T30 to T42). Croziers are dikaryotic because they contain two
277 haploid nuclei derived from both parents. Karyogamy (T30 to T44) occurs in the
278 upper cells of croziers. The resulting diploid zygote immediately undergoes meiosis
279 (T30 to T44), producing four haploid nuclei, which then undergo mitosis prior to
280 ascospore delineation (T54 to T96). Ascospores are formed around two non-sister
281 nuclei within the developing asci. In rare cases, two ascospores form around a single
282 haploid nucleus, resulting in five-spored asci. **C.** Time line of the sexual cycle of *P.*
283 *anserina* with the steps from which RNAs have been extracted on the left.
284
285 *P. anserina* is a pseudohomothallic fungus, namely natural isolates are self-fertile
286 because they contain nuclei of each mating-type. Self-fertilization does not start at a specific
287 time point and therefore natural isolates cannot be used for a time course analysis of sexual
288 development. However, the genetic basis of the *P. anserina* mating system is heterothallism
289 with two mating-type idiomorphs called *mat*+ and *mat*- (Turgeon and Debuchy 2007). Typical
290 ascospores contain *mat*+ and *mat*- nuclei, but a few asci contain monokaryotic ascospores
291 which produce self-sterile individuals. Those latter individuals were used in the experiments
292 presented here. Fertilization was performed by spreading *mat*- male gametes on a *mat*+ strain.
293 This experimental design allows the time course to start at a well determined time point for
294 synchronization purpose. Under this experimental condition almost all fertilization events
295 occurred within the first six hours (Fig. S2A and S2B). However, despite this experimental
296 design, RNA samples were extracted from biologically non-homogeneous tissues because *P.*
297 *anserina* fructifications are composed of different cell types (Fig. 1A and 1B).
298 We measured the expression of 10,507 nuclear genes at ten time points which are
299 designated as Tm24 for mycelium 24 h before fertilization and T0, T6, T12, T18, T24, T30,
300 T42, T54 and T96 for time 0 to 96 h postfertilization, respectively (Fig. 1C, Table S1). We
301 performed a Principal Component Analysis (PCA) on the complete dataset. More than 75% of

302 the total variance was captured by only three principal components (PCs, Fig. 2A and 2B, Table
303 S2).

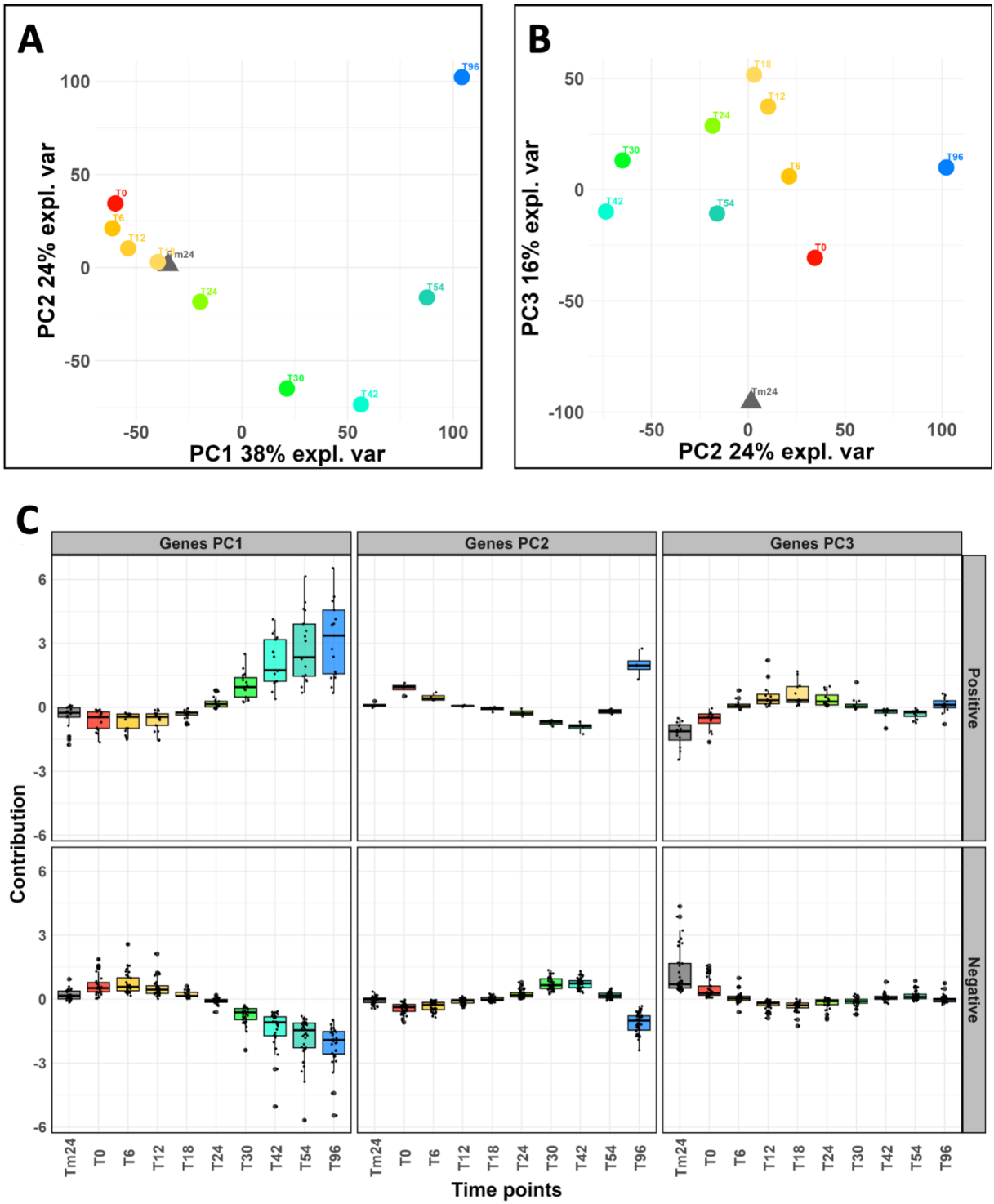

304

305 **Figure 2 - PCA analysis reveals a strong temporal effect on gene expression**
306 **variations relevant to the key developmental steps in *P. anserina***
307 Principal Component Analysis (PCA) on the complete dataset (*i.e.* all gene
308 expression profiles, see Methods). **A.** Axis 1 and 2 of the PCA explain 38% + 24 %

309 = 62% of the variance. **B.** Axis 2 and 3 of the PCA explain 24% + 16 % = 40 % of
310 the variance. Altogether, these first three axes of the PCA explain 78 % of the
311 variance. **C.** Gene expression profiles for the 50 genes, which contribute the most to
312 the definition of the first (PCA1), second (PCA2) and third (PCA3) principal
313 components, as shown in A and B. Detailed lists of these genes are given in Table
314 S2. They were separated according to the type of regulation they experience during
315 sexual development (positive or negative). Tm24, T0, T6, T12, T18, T24, T30, T42,
316 T54 and T96 : time points of the kinetic were the biological samples were collected,
317 described in Fig. 1.
318
319 With the exception of Tm24, we observed that all samples were distributed along the
320 PC1 axis (38%) according to the sexual development time line (Fig. 2A). On PC2 axis, we
321 found T30 and T42 samples clustered apart from the others (24%). Interestingly, this period
322 corresponds to the formation of the dikaryotic cells, which are the progenitors of fungal zygotic
323 lineage (Fig. 1). The peripheral position of the Tm24 sample (Fig. 2B) which appeared on the
324 PC3 axis (16%), indicated that the gene expression profiles derived from vegetative mycelium
325 (Tm24) were clearly different from those of all samples collected after fertilization. Overall,
326 this unsupervised exploratory data analysis validated both the relevance of our experimental
327 design and the robustness of our differential analysis (see below). The expression profiles for
328 the 50 genes whose expression measurements contributed the most to the calculation of the
329 principal components 1, 2 and 3 are shown Figure 2C (and detailed Table S2). The data
330 indicated that the greatest fold changes, both positive and negative, occurred after the formation
331 of dikaryotic cells (>T30). This was also the case for PC2, but only after the formation of the
332 ascospores (>T54). We observed that the positive fold change values on PC1 exhibited a higher
333 dispersion after T42.
334 **Topology of global expression variation reveals five major transcriptional waves during**
335 **sexual development**
336 Using k-means clustering, we defined 13 representative expression patterns (Fig. S1 and
337 Fig. S3), encompassing 1,186 genes. Further data integration outlined five successive
338 transcriptional waves (Fig. 3, Fig S1 and Table S1). Notably, they all shared a common pivot
339 point (Fig. S4), corresponding to the mid-course of the kinetic (T30-T42). This observation
340 indicated a pause in the regulation of transcriptional activity at the time of dikaryon formation.
341 The 1,186 genes were not evenly distributed across the five waves (Fig. 3 and Table S1),

342 resulting in two periods of intense and equal transcriptional fluctuation (waves II and IV)
343 interspersed with three periods of moderate transcriptional fluctuation (waves I, III, and V).

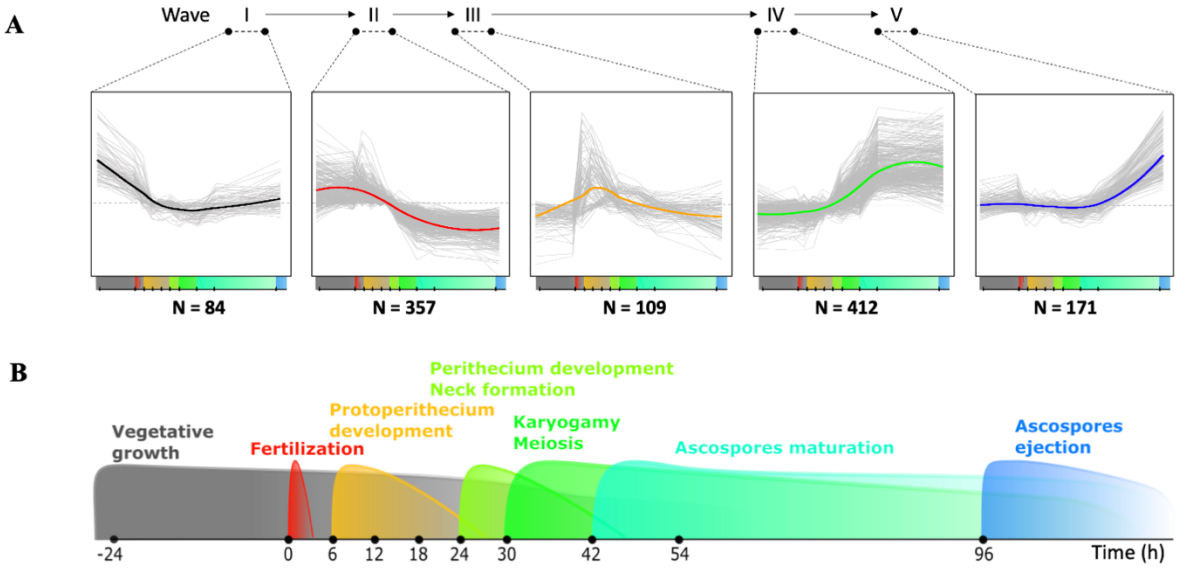

344

345 **Figure 3 - Temporal transcriptional waves over the course of sexual**
346 **development**

347 **A.** Expression profiles of the five major successive transcriptional waves (numbered
348 in Roman figures) that take place during *P. anserina* sexual reproduction (Bottom
349 timeline, see panel B for zoom). Number of differentially expressed (DE) genes
350 present in each wave is indicated below the corresponding graph. Waves II (early
351 up/late down pattern, 31.51%) and IV (early down/late up pattern, 36.37%)
352 accounted for 67.87% of them (33.98% and 37.42%, respectively), while wave I
353 (early down pattern, 7.41%), wave III (early-mid up pattern, 9.62%) and wave V
354 (late up pattern, 15.02%) contained only 32.13% of them, respectively.

355 **B.** Major developmental events according to the sexual reproduction timeline
356 described in Figure 1.

357

358 The topology of the transcriptional waves therefore suggests that the genes of waves II
359 and III are down-regulated after a peak of expression during protoperithecium development,
360 while the genes of waves IV and V are up-regulated after perithecium development. These
361 patterns are in accordance with the results obtained in *N. crassa*, during fruiting body
362 development (Wang *et al*. 2014).

363 **Evolutive conservation and functional annotation of differentially expressed genes during**
364 **sexual reproduction**

365 Across the entire time-course experiment, we found 3,466 genes that were differentially
366 expressed (DE, see Methods). They represent 33% of the total gene set for which gene
367 expression measurements were monitored (Table S1, Fig. 4A), including 1,133 of the genes
368 clustered in the five transcriptional waves (more than 95% of the clustered genes, Table S1 and
369 Fig. 3 and Fig. S1). Overall, this analysis revealed that in *P. anserina*, one-third of the complete
370 gene set is transcriptionally regulated during sexual reproduction. Of this, one-third follows one
371 of the five transcriptional waves disclosed by the clustering analysis. To test for evolutive
372 conservation of these DE genes, we built group of orthologs (see Methods), using four species
373 of filamentous fungi, *i.e*. the homothallic species *Chaetomium globosum* and *Sordaria*
374 *macrospora* and the heterothallic species *N. crassa* and *Trichoderma reesei*. A total of 2,957
375 DE genes (more than 85%) were identified as belonging to an ortholog group shared with at
376 least one of the four species (Table S3). A core set of 1,496 DE genes is conserved in all four
377 fungi (Fig. 4, Table S3).

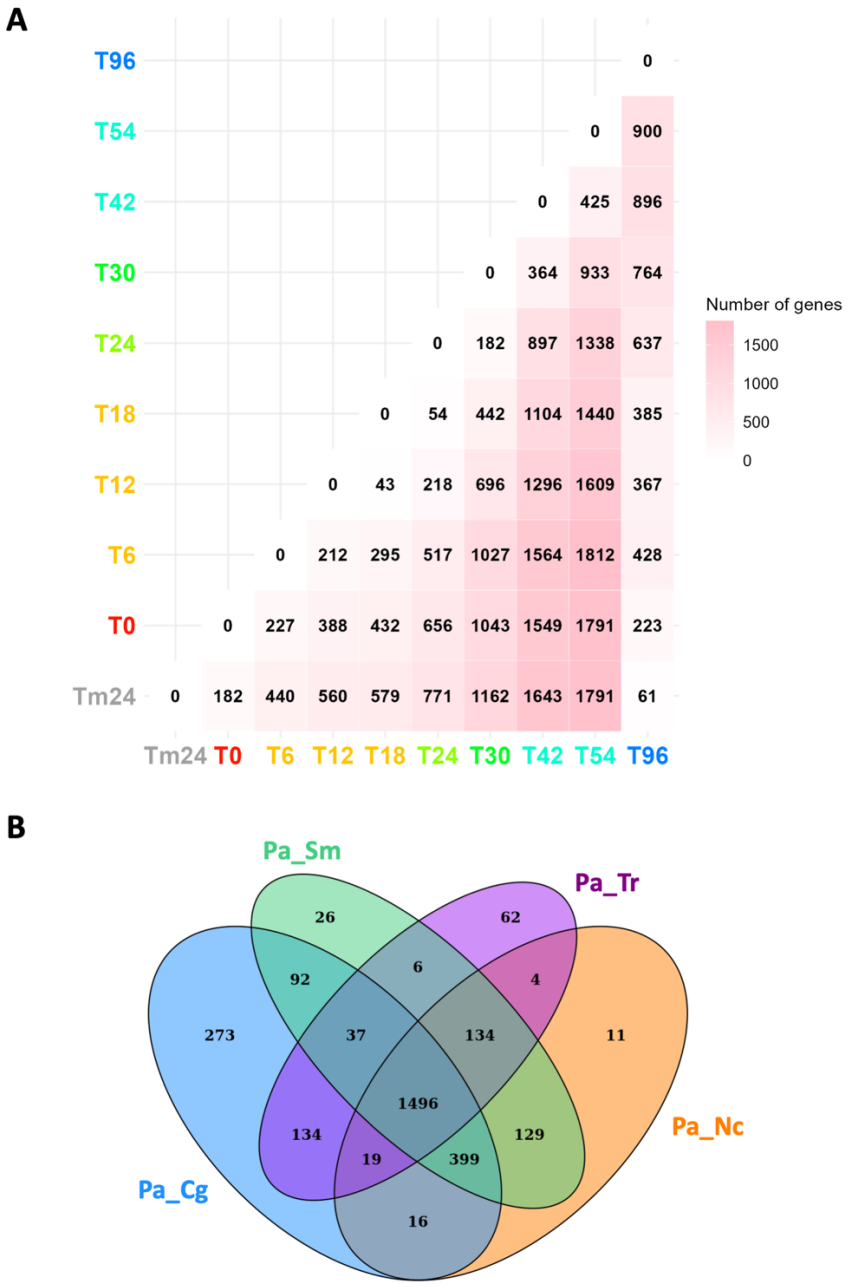

Figure 4 - Distribution of differentially expressed genes along the kinetics of sexual reproduction and their evolutive conservation

A. Heatmap of pairwise comparisons of differentially expressed (DE) genes across the complete time-course experiment. Numbers correspond to the numbers of genes with an adjusted p-value lower than 0.001 and an absolute fold change value between the two compared time points, higher than 2 (see Methods).

B. Venn diagram showing the conserved orthologs between the indicated fungal species. Cg: *C. globosum* (homothallic), Sm: *S. macrospora* (homothallic), Nc: *N. crassa* (heterothallic) and Tr: *T. reesei* (heterothallic).

A pairwise comparison of the DE gene set of *P. anserina* with each gene set of the four fungi, showed that the number of conserved DE genes is consistent with fungal evolutionary history. Closely related species (*C. globosum*) share more DE genes than the more distantly related species (*N. crassa*, *S. macrospora* and *T. reesei*). The remaining 506 genes (14.78%) were classified as orphan genes, with 247 (21.84%) belonging to the five transcriptional waves. Notably, the set of DE genes, including that of the five waves, were found to be enriched with orphan genes (p-values: 2.55×10^{-9} and 4.60×10^{-20} respectively).

We then search for functional annotation of the proteins encoded by the DE genes (see Methods). We found that 1,279 (36.95%) of the 3,466 putative proteins encoded by the DE genes lacked Pfam annotation (Table S1, (Mistry *et al*. 2021)), which is significantly more (p-value: 8.55×10^{-9}) than in the complete list of *P. anserina*'s proteins. The lack of annotated conserved domains was further enriched (p-value: 1.48×10^{-13}) in wave-embedded DE genes, as 515 out of these 1,133 putative proteins (45.44%) lacked Pfam annotation. We also performed Gene Ontology (GO, (Ashburner *et al*. 2000; The Gene Ontology Consortium *et al*. 2023)) analysis on the DE genes (Table S4, Fig. 5A).

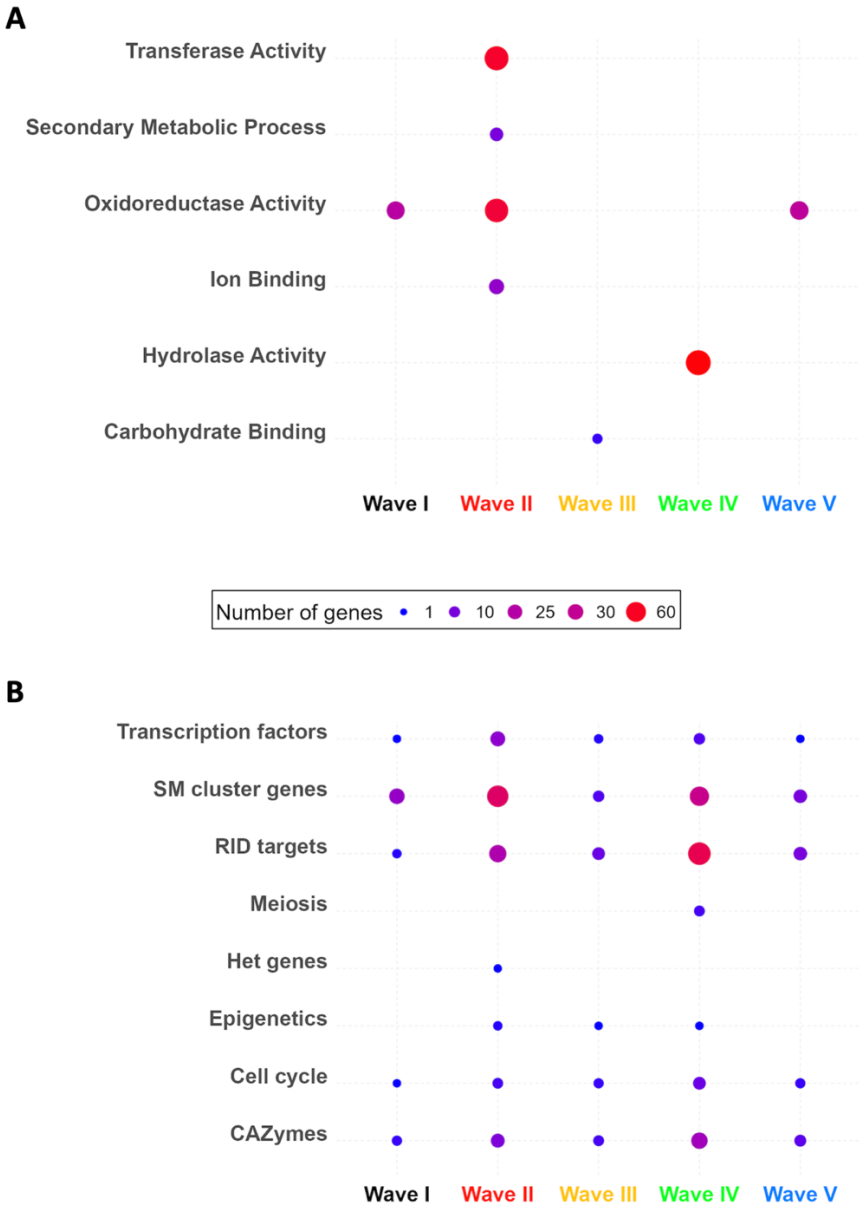

Figure 5 - GO term and expert annotation categories enriched in the transcriptional waves.

A. Descriptions of GO terms significantly enriched (p-value ≤ 0.05) in at least one wave of the transcriptional waves. **B.** Enrichments of genes of interest in at least one wave of the transcriptional waves. TF: transcription factors, SM: secondary metabolites, HET: fungal specific vegetative incompatibility HET domain. Points are scaled and colored according to the number of genes in each category for each wave. No score is shown for zero genes.

In general, the enriched GO terms and Pfam domains (Table S4 and S5) described intense catalytic (GO:0003824) and metabolic (GO:0008152) activities, associated with binding (GO:0005488, PF00187). Accordingly, we observed enrichments in genes involved in

417 redox catalytic activities (GO:0003824, PF00067, PF03055, PF01565, PF00106, PF01494,
418 PF00199, PF08240) and transporter activities (GO:0005215, Pfam PF07690.19). We also
419 uncovered enrichments in DE genes involved in cellular differentiation programs more
420 specifically related to sexual reproduction. They either deal with cellular anatomical entity
421 (GO:0110165), localization (GO:0051179) or encode zinc-binding domain transcription factors
422 (PF13695), necrosis inducing factor (PF14856) and TUDOR domain containing protein
423 (PF11160). However, if the repertoire of GO terms (Table S4) and Pfam domains (Table S1
424 and S5) generated by this study should provide some clues to select candidate genes for *in vivo*
425 functional characterization, our analysis essentially showed that more than one third of the DE
426 genes have no associated function yet.

427 **Searching for genes of interest, the expertise-driven approach**

428 We then performed a biological expertise-driven approach to mine the functions of the
429 full set of DE genes (Table S6, Fig. 5B).

430 **. Developmental processes at work**

431 Fertilization of *P. anserina* requires exposure to blue light, but the molecular basis of
432 this signal transduction is still unknown. In *N. crassa*, the blue light signal is transduced by the
433 photoreceptors WC-1 and WC-2 (Froehlich *et al*. 2002; He *et al*. 2002). In this study, we found
434 five blue light responsive genes that were differentially expressed (Table S6A, Fig. S5A-B).
435 Consistent with a role in fertilization three of them (including *Pa_ 5_6130/WC-1*) were
436 expressed before meiosis, while the other two were expressed after meiosis, suggesting that
437 blue light may also play a role during ascospore formation.

438 Orthologs of genes involved in plasmogamy in yeast models (*Pa_3_11320/Prm1* (Curto
439 *et al.* 2014*)*, *Pa_3_4770/CDC3* (Kurahashi, Imai, and Yamamoto 2002), *Pa_5_9510/Fig1*
440 (Erdman *et al*. 1998), *Pa_1_1930/KEX2* (Julius *et al*. 1984), *Pa_4_6420/KAR2* (Rose, Misra,
441 and Vogel 1989), *Pa_7_10810/SEC63* (Young *et al*. 2001) were found to be up-regulated until
442 T42 and then downregulated (Table S6A, Fig. S5C). Development of the zygotic lineage likely
443 involves compartmentalization through active cell wall remodeling, as we found several DE
444 genes encoding different types of cell wall proteins and growth factor receptors (Table S6A).
445 One of them was the expansin-like EEL2, involved in cell wall expansion, whose gene
446 *Pa_2_310* was downregulated from karyogamy to ascospore maturation (T30-T96). This
447 expression pattern was similar to that of the C. *globosum* homolog (*CHGG_00523*) but
448 divergent from that of the *N. crassa* homolog (*NCU04603*) (Hutchison and Glass 2010; Wang
449 *et al*. 2019). Cell-cell interactions may also be tightly regulated, as exemplified by the strict

450 downregulation (T0-T96) of *Pa_1_17480,* which encodes the adhesin protein MAD1 (Wang
451 and St Leger 2007).
452 Since sexual development is rich in cell divisions, we searched for DE cell cycle related
453 genes and found this category slightly enriched (p-value = 2.9×10^{-2}, Table S5B). In addition to
454 the TOR pathway inhibitor *Pa_3_3700/FgFkbp12*, it included homologs of genes required for
455 proper fructification formation (*Pa_1_17170/KIN3*, *Pa_1_23300/cel-2*, *Pa_2_6460/Pah1*,
456 *Pa_2_890/asm-1*), axial budding (*Pa_2_290*/*axl2*) and genes encoding G-coupled receptors
457 (*Pa_4_5350*, *Pa_1_590*) and ras-like protein (*Pa_1_19030*/*krev-1*). The expression profile of
458 the *Pa_2_290*/*axl2* gene, encoding an integral plasma membrane protein, was of particular
459 interest: it was down-regulated when the two haploid parental nuclei actively divide into
460 multinucleated syncytial ascogonial cells (Fig. S5D).
461 As expected, we also found DE genes encoding cytoskeletal elements (Fig. S5E).
462 Interestingly, *Pa_5_5720*, encoding a pyruvate decarboxylase (PDC) was found strongly up-
463 regulated during ascospore maturation (wave V). This observation further enforces the
464 hypothesis that pyruvate decarboxylase is involved as a structural protein (PDC-filaments)
465 associated with the cytoskeleton during the sexual development of filamentous fungi
466 (Thompson-Coffe *et al*. 1999). Conversely, *Pa_4_7260*, encoding the nucleoprotein Cik1,
467 required for both karyogamy and mitotic spindle organization (Cottingham *et al*. 1999), was
468 found down-regulated at the same time. Some of the cytoskeleton DE genes showed co-
469 expression with the plasmogamy DE genes (Fig. S5F), making them good candidates to be
470 involved in fusion morphogenesis processes.
471 Three genes essential for ascus development were also found DE (Fig. S5G, Table S6A):
472 *P. anserina*'s orthologs of *Pa_4_9730/asd-1* (wave IV (Nelson, Merino, and Metzenberg
473 1997)), *Pa_4_9750/asd-3* (Galagan *et al*. 2003) and *Pa_2_13270/con-6* (wave V (White and
474 Yanofsky 1993)). *P. anserina* does not form clonal propagules. However, the orthologs of genes
475 required for conidiation in *N. crassa* and *Aspergillus nidulans* such as *Pa_2_13270/con-6*,
476 *Pa_4_9730/asd-1*, *Pa_4_9750/asd-3, Pa_1_12720/Pyg1*, *Pa_1_30/TmpA* and *Pa_0_1540*
477 were found to be up-regulated after meiosis, suggesting that genes primarily involved in
478 conidiation, *i.e.* asexual reproduction, may have been recruited to participate in ascospore
479 formation. On the contrary, early conidial development-2 *Pa_7_780/ecd-2* was down regulated
480 during the first half of the kinetic (Sun *et al*. 2012).
481 **. Producing energy**
482 The reproductive process is energy consuming and therefore the mobilization of carbon
483 resources is one of the keys to its success. The genome of *P. anserina* contains 276 genes

484 encoding CAZymes ((Espagne *et al*. 2008) and Table S6D). Among them, 141 were found DE
485 during sexual development, showing an enrichment of this metabolic activity (p-value =
486 $4.36x10^{-5}$). The expression profile of 42 CAZyme genes corresponded to one of the five
487 transcriptional waves, especially waves II and IV. The remaining 99 showed contrasting
488 expression patterns (Fig. S5 H-T), but up-regulation was enriched over down-regulation, as 62
489 of them were up-regulated during the kinetic (Chi^2, p-val < 0.001). We also found that several
490 CAZymes genes had some of the highest positive fold changes measured in this study (Table
491 S1). In addition, three glycolysis enzymes genes (6-phosphofructo-2-kinase *Pa_3_6610*,
492 fructose-bisphosphate aldolase *Pa_0_710*, and phosphoglycerate kinase *Pa_6_10610*) were up-
493 regulated with a similar pattern of overexpression when asci begin to differentiate (Fig. S5U,
494 Table S6E).

495 In *P. anserina*, long-chain fatty acids are shortened in peroxisomes then degraded in
496 mitochondria. The *Pa_6_3500*/*PaPex7* gene, which encodes the peroxisomal-targeting-signal-
497 2 receptor, is found to be up-regulated during ascospore maturation (T54-T96, Table S1 and
498 Fig. S5V). This is in line with the defects in nuclear positioning of the post-meiotic asci
499 observed in *pex7* knock-out mutants, which can result in either abnormal ascospore formation
500 or to ascospores containing an abnormal number of nuclei (Bonnet *et al*. 2006). The
501 *Pa_1_23790*/*PaFox2* gene (Table S1 and Fig. S5V), which encodes the peroxisomal
502 multifunctional protein 2, a key enzyme in the fatty acid ß-oxidation pathway, was found to be
503 down-regulated during the early stages of sexual development (T12-T54) and up-regulated
504 during ascospore maturation (T54-T96). This expression profile may explain the reduced
505 acetyl-CoA availability within the ascospores that results in the pigmentation defect observed
506 in *PaFox2* knock-out mutants (Boisnard *et al*. 2009).

507 **. Secondary metabolites: major actors of sexual development?**

508 Prokaryotic and eukaryotic micro-organisms produce a wide variety of secondary
509 metabolites (SMs). These molecules are not intended to perform housekeeping functions, but
510 rather are used as adaptive tools to cope with environmental fluctuations or to compete with
511 other living organisms. The *P. anserina* genome contains 35 biosynthetic gene clusters (BGCs)
512 (Lamacchia *et al*. 2016), Table S6F, Fig. S5W), containing 474 genes. SM encoding genes were
513 enriched among the complete set of DE genes (p-value = $8.31x10^{-10}$) as 258 of them were found
514 to be DE (33 out of 35 BGCs contained at least two DE genes). These genes were also
515 significantly up-regulated (Chi^2, p-val < 0.001). BGCs N°1, 11, 18, 19, 24, 27 and 34 showed
516 an expression profile topology (Fig. S5W) similar to the general pattern described in *N. crassa*

517 (Wang *et al*. 2022), which was a coordinated downregulation from fertilization to meiosis
518 followed by a coordinated upregulation during ascospore formation and maturation.
519 We also examined whether co-expression was shared by multiple SM genes within the
520 34 BGCs. This was the case for the sterigmatocystin BGC, where 17 of the 23 genes were
521 differentially expressed during sexual reproduction (Table S6F, cluster 32, Fig. S5X, (Slot and
522 Rokas 2011)), including the transcription factor *PaAflr* (Shen *et al*. 2019). In addition, we
523 identified four positive regulators of the sterigmatocystin BGC (Table S6F, Fig. S5Y,
524 *Pa_2_7220, Pa_2_7240, Pa_2_7250, Pa_2_7260* (Bhetariya *et al*. 2011)), that showed the
525 same expression pattern across sexual reproduction. Similarly, 13 of the 20 genes in the
526 terrequinone BGC were differentially expressed (Fig. S5Z).
527 In addition, we identified several isolated genes from different BGCs that showed
528 similar peak expression to each other but no co-expression with other genes from their
529 respective BCG (Fig. S5AA-AB). These expression peaks of genes encoding mostly proteins
530 of unknown function corresponded to two key moments in early development (T6 and T12),
531 just before and during dikaryon formation. Taken together, our analyses further support the key
532 role of SM in sexual reproduction and highlight the role of previously uncharacterized clusters
533 and isolated SM genes.
534 **. From regulation of biotic interactions to that of sexual development**
535 Genes encoding STAND proteins (Signal-transducing ATPases with Numerous
536 Domains, (Leipe, Koonin, and Aravind 2004) have been described as involved in fungal biotic
537 interactions with living organisms, either from the same species or from different species but
538 mostly during vegetative growth. The *P. anserina* genome contains 34 genes encoding STAND
539 proteins with a NACHT domain (PF05729), eight of which were found to be down-regulated
540 either throughout the sexual cycle kinetics or prior to perithecium development (Table S6G,
541 Fig. S5AC). This group includes *Pa_3_10930*/*nwd1* (Chevanne *et al*. 2010), *Pa_7_10370*/*sesB-*
542 *like*, *Pa_2_7940*/*het-d* (Espagne *et al*. 2002) and *Pa_1_11380* (Bidard, Clavé, and Saupe 2013).
543 Fungal interactions are also under the control of a programmed cell death called vegetative
544 incompatibility that prevents hyphal fusion of two genetically distinct wild-type strains. Most
545 of the effectors of this incompatibility reaction (IR) contain HET domains (PF06985).
546 Strikingly, 59 of the 128 *het* genes annotated in the *P. anserina*'s genome were found to be DE,
547 including *Pa_4_1190*/*hnwd1* and *Pa_7_3460*/*Pin-C* (Chevanne *et al*. 2010; Kaneko *et al*. 2006;
548 Bidard, Clavé, and Saupe 2013). The majority of the DE *het* genes were down-regulated either
549 throughout the complete sexual development or from dikaryon formation (Fig. S5AD), but
550 seven of them were up-regulated during some steps of the kinetic, mostly after karyogamy (Fig.

551 S5AE). In addition, three *het* genes showed a peculiar behavior (Fig. S5AF): *Pa_5_2540*
552 expression oscillated during sexual reproduction, *Pa_3_5550* expression peaked during
553 protoperithecium development and *Pa_4_1800* expression was down-regulated until ascospore
554 maturation and over-expressed during this process.

555 In the DE gene set, we also found gene families encoding toxins that can induced host
556 cell death or effector-like proteins. All of the six genes encoding the NEP1-like proteins pore-
557 forming toxin NPP1 (necrosis-inducing *Phytophthora* protein, (Ottmann *et al*. 2009) were
558 down-regulated at least during the second half of the sexual development, i.e. before karyogamy
559 (Fig. S5AG). Six out of the eight genes encoding Hce2 pathogen effectors (Stergiopoulos *et al*.
560 2013) and one gene annotated as Ptu bug toxin encoding gene (*Pa_6_9450*) were also DE. In
561 contrast to the *NPP1* genes, all of them showed up-regulation during the course of sexual
562 development, five of them belonging to the wave IV pattern of expression (Fig S5AH).

563 **. Epigenetic effectors at work in sexual reproduction**

564 In recent years, epigenetic effectors have been identified as key players in fructification
565 morphogenesis (Carlier *et al*. 2021; Nowrousian 2022). Therefore, we investigated the
566 expression patterns of genes encoding proteins that can either methylate cytosines, write or
567 erase histone post-translational modifications or interfere with messenger RNA synthesis and
568 stability.

569 *PaRid* and *PaDnmt5*, two of the three DNA methyltransferase encoding genes present
570 in the *P. anserina* genome, were found to be DE during this time-course experiment. *PaRid*
571 expression, which is essential for dikaryon formation (Grognet *et al*. 2019) peaked at T12, while
572 *PaDnmt5* expression was increasingly up-regulated from T12 to T42 (Fig. S5AI). *Pa_5_2900*,
573 which encodes a RING-type E3 ubiquitin transferase URF1-like, was found to be strongly up-
574 regulated from T42. In mammals, this protein binds both hemi-methylated DNA and tri-
575 methylated lysine 9 of histone H3 (H3K9me3), thereby bridging DNA methylation and
576 chromatin modification (Foster *et al*. 2018).

577 *Pa_7_10020*/*KAT1* and *Pa_1_7460*/*Hos-2* encodes two chromatin modifiers with
578 antagonistic enzymatic activities, respectively a histone acetyltransferase encoding gene (Tong
579 *et al*. 2012) and a histone deacetylase (Wang, Kurdistani, and Grunstein 2002) respectively.
580 However, these two genes showed co-expression over the entire kinetic, *i.e*. they were up-
581 regulated from fertilization to karyogamy and then down-regulated (Fig. S5AJ). This pattern
582 was in contrast to that of *Pa_7_5890* encoding the Sin3-associated polypeptide SAP18, which
583 enhances transcriptional repression through histone deacetylation (Cheng and Bishop 2002).
584 Two genes encoding sirtuins NAD(+)-dependent histone deacetylases were also found to be

585 DE: *Pa_4_8570*/*PaSir2* showed a wave III expression pattern that resembled that of
586 *Pa_1_19440*/*PaRid* (Fig. S5AI), while the gene encoding *Pa_4_7390*/*SIRT5* was down-
587 regulated throughout sexual reproduction. Of the 32 genes encoding SET domain proteins,
588 seven were found to be DE (Fig. S5AK), although none has yet been shown to have histone
589 lysine methyltransferase activity. Four genes encoding putative histone demethylase containing
590 JmJC domains were also found DE (Fig. S5AL).

591 Promoter accessibility also depends on nucleosome positioning. The ATP-dependent
592 chromatin remodeling protein SWI/SNF *Pa_5_4310/SMARCA3* (Oh *et al*. 2013) was one of the
593 most highly up-regulated wave III genes (Fig. S5AM). Its transcription pattern is similar to that
594 of *Pa_1_19440*/*PaRid* (see Fig. S5AI) and *Pa_4_8570*/*PaSir2* (Fig. S5AJ). Transcription
595 requires a large number of proteins assembled into conserved complexes. Two genes
596 (*Pa_1_17860* and *Pa_6_1460*) encoding components of the SAGA complex were found to be
597 up-regulated from T6 to T54 with very similar expression patterns (Fig. S5AM). However, we
598 also found similarly co-regulated genes although encoding factors with antagonistic effects on
599 transcription, such as the SWD2 subunit of the COMPASS complex (*Pa_7_11070*) and the
600 extra sexcombs subunit of the Polycomb Repressive Complex 2 (*Pa_3_4080*).

601 There is no experimental evidence that post-transcriptional RNAi mechanisms Quelling
602 (Romano and Macino 1992) and MSUD (Shiu *et al*. 2001) are functional in *P. anserina*.
603 However, genes encoding essential components of Quelling (Fig. S5AN), the RNA-dependant
604 RNA polymerase (RdRP) *Pa_7_4790/Qde1* (Cogoni and Macino 1999) and the dicer
605 *Pa_6_6150/Dcl-1* (Yang, Ye, and Liu 2015), were downregulated from T18 and T30,
606 respectively. On the contrary, expression of *Pa_7_9210* encoding the Qde-2 interacting
607 exonuclease QIP was up-regulated from T6 to T30. *N. crassa* Δ*qde-1* quelling mutant strains
608 produced normal-sized perithecia but no ascospore (Wang *et al*. 2014). Four genes involved in
609 MSUD were also found to be DE (Fig. S5AO). *Pa_2_9830*/*Sad-2* and *Pa_5_11380*/*Sad-5* were
610 up-regulated whereas *Pa_1_19900*/*Sad-1*, encoding the RdRP and *Pa_1_16040*/*Sad-3*,
611 encoding the helicase, were down-regulated. Interestingly, *Pa_6_11690*/*rrp-3*, which encodes
612 an RdRP that could not be clearly assigned to Quelling or MSUD pathways in *N. crassa*
613 (Borkovich *et al*. 2004), was co-expressed with the Quelling genes *Pa_1_19900*/*Sad-1* and
614 *Pa_1_16040*/*Sad-3* in *P. anserina*. Knockout of the *N. crassa Sad-1* and *Sad-3* resulted in arrest
615 of ascus development in meiotic prophase and production of normal-sized perithecia and young
616 asci without ascospores, respectively (Wang *et al*. 2014). *Sad-2* is essential to *N. crassa*
617 fructification development (Wang *et al*. 2014). These results suggest that RNAi genes may be
618 silenced during meiosis and sporulation, which may explain the apparent lack of MSUD in *P.*

619 *anserina* but also that *Pa_2_9830*/*Sad-2* and *Pa_5_11380*/*Sad-5* might have been recruited to
620 play a role during ascospore dormancy.

621 Repeated sequences present in both haploid parental genomes of *P. anserina*'s
622 dikaryotic cells are subjected to cytosine-to-thymine mutations by repeat-induced point
623 mutation (RIP, (Bouhouche *et al*. 2004)). Modified 5-methylcytosines are known to be hotspots
624 for cytosine-to-thymine transitions, because, unlike unmethylated cytosines, spontaneous
625 deamination of 5-methylcytosines cannot be repaired by uracil excision (Pearl 2000). To
626 counteract this genetic threat, members of the AlkB alpha-ketoglutarate-dependent dioxygenase
627 (PF13532) family oxidize 5-methylcytosines to restore undamaged bases (Bian *et al*. 2019).
628 Two genes encoding AlkB-like enzymes are present in the *P. anserina* genome. The expression
629 of *Pa_1_12280* was down-regulated throughout the kinetic, while *Pa_1_17260* was up-
630 regulated during two segments of the kinetic: i) from Tm24 to T12, corresponding to the peak
631 of expression of *PaRid* and ii) from T24 to T54, when *PaRid* is no longer expressed (Fig.
632 S5AP). Notably, both genes showed a superimposable flat expression profile at the time of RIP.

633 In filamentous fungi, a conserved post-transcriptional A-to-I mRNA editing process
634 recodes transcription units (Teichert *et al*. 2017; Blank-Landeshammer *et al*. 2019), mainly
635 during fructification and ascospore morphogenesis. We identified seven DE genes encoding
636 adenosine deaminase acting on tRNA (ADAT), a class of enzymes which are responsible for
637 A-to-I mRNA editing. *Pa_1_21170*, a wave III gene, showed a peak of expression similar to
638 that of *PaRid*, while *Pa_3_6600* and *Pa_6_7750* were up-regulated from perithecium
639 development to ascospore discharge (Fig. S5AQ).

640 **Co-expression Network: In Search of Potential Transcription Factor Targets During**
641 **Sexual Reproduction**

642 We then focused on the 96 TFs encoding genes that were found to be DE (Table S6I).
643 The expression profile of each TF gene was used to search for significant correlations with the
644 expression profiles of all genes previously classified as transcriptional waves I, II, III, IV or V
645 (see Methods). Using this strategy, we build a network of 2002 potential transcriptional links
646 between 76 TFs and 683 target genes (Fig. 6 and Table S7A-C).

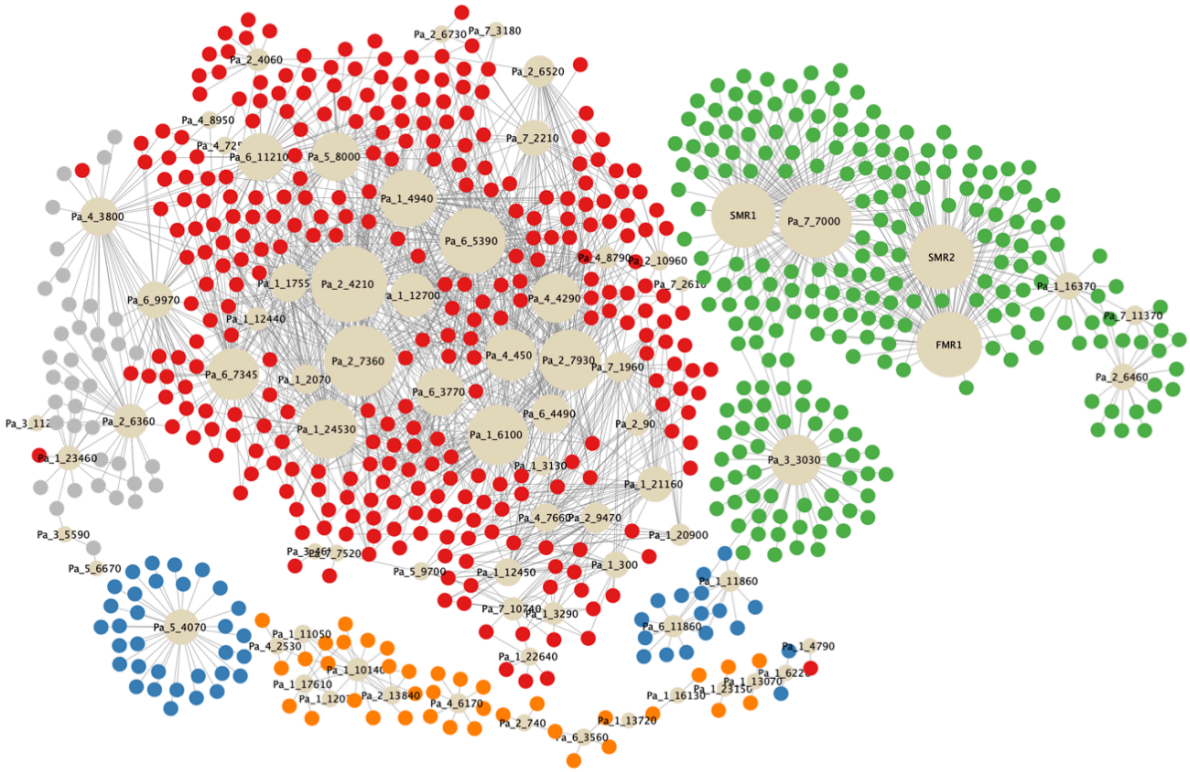

Figure 6 - Co-expression network based on expression profiles of differentially expressed (DE) genes coding for transcription factors

Genes encoding transcription factors (TF) are represented by beige circles whose size represents the number of co-regulated genes. These coregulated genes, which can be considered as potential TF target genes, were classified in transcriptional waves as such: wave I: grey color (61 genes), wave II: red color (1402 genes), wave III: orange color (58 genes), wave IV: green color (426 genes) and wave V: blue color (55 genes).

Some of the prominent nodes of this network were expected TFs (FMR1, SMR1, SMR2, Pa_1_10140/Pro1, see below), confirming its relevance. However, most of the 76 TFs (72%) had no characterized biological function, including those with the broader set of target genes. The distribution of the TFs encoding genes in the five transcriptional waves differed from that of the total set of DE genes (Fig. 6), with the majority belonging to wave II. As with TFs, most of the target genes were of unknown function. Importantly, some TFs were also target genes, e.g. *Pa_1_10140/Pro1*is a target of Pa_1_12070/HOM3Pa_1_11050/HMG4, Pa_1_17610, and Pa_2_13840 (Table S7A).

Among the master regulators of this network, we identified HMG-domain and homeodomain TFs (Espagne *et al*. 2008; Ait Benkhali *et al*. 2013). The HMG-domain TFs

667 include the mating-type proteins FMR1 and SMR2, which are both required for the
668 development of the perithecium after fertilization (Zickler *et al*. 1995; Arnaise *et al*. 2001).
669 Physical interaction between FMR1 and SMR2 was demonstrated and proposed to be required
670 for their post-fertilization functions (Arnaise *et al*. 1995; Turgeon and Debuchy 2007; Bidard
671 *et al*. 2011). Our study shows that FMR1 and SMR2 have a similar expression profile
672 throughout sexual reproduction (Fig. S5AR). Their co-expression networks revealed also an
673 almost identical number of potential target genes (FMR1, n = 79; SMR2, n = 78) (Table S7).
674 They share 62 of their 79 potential target genes (Table S7A). These observations support the
675 idea that they act together in identical regulatory pathways by forming a heterodimer (Arnaise,
676 Debuchy, and Picard 1997). The third and last *mat*- mating-type gene, *SMR1*, does not belong
677 to the HMG-box family. It encodes a HPG protein (Turgeon and Debuchy 2007), which has
678 been proposed to provide a scaffold for physical interaction of mating-type proteins *(Zheng et*
679 *al*. 2013). This role is consistent with its presence in wave IV, along with *FMR1* and *SMR2*
680 (Fig. S5AR). Critical genes for the development of ascogenous hyphae are likely to be found
681 among target genes of FMR1, SMR2 and SMR1 (Fig. 6, Table S7A). The only non-mating-
682 type HMG protein present in the network is Pa_1_11050/PaHMG4, related to Nhp6p and
683 Hmo1p from *S. cerevisiae* (Ait Benkhali *et al*. 2013). Its deletion in *P. anserina* resulted in an
684 increased number of male organs. The lack of effect on fructification development is consistent
685 with the down-regulation of *Pa_1_11050/PaHMG4* at T42-T96 (Fig. S5AS). Proper shaping
686 of the developing fructifications requires the homeobox protein *Pa_2_6460/Pah1* (Coppin *et*
687 *al*. 2012). The expression of the corresponding gene was accordingly up-regulated from T0 to
688 T42 (Fig. S5AS). In contrast, *Pa_3_4650/Pah6* was down-regulated between T0 and T54 (Fig.
689 S5AS), although no fructification defect was associated with its deletion.
690 The $Zn(II)_2Cys_6$ class of regulators is one of the largest families found in fungi
691 (MacPherson, Larochelle, and Turcotte 2006) and consequently they represented almost half of
692 the TFs present in the network (Table S7A). Three of them are of particular interest and have
693 been extensively studied because of their properties. *Pa_1_10140/PaPro1* is a regulator of the
694 expression of the mating-type and *IDC* genes, both required for female fertility (Gautier *et al*.
695 2018). In *S. macrospora*, *Pro1* has been identified as a master regulator of fructification
696 formation (Steffens *et al*. 2016; Teichert, Pöggeler, and Nowrousian 2020). Its temporal and
697 spatial expression is consistent with the presence of *Pa_1_10140/PaPro1* in wave III (Fig.
698 S5AS). *Pa_7_7000* was characterized in wave IV as a coregulator of FMR1, SMR2 and SMR1
699 target genes (Fig. 6). *Pa_7_7000* is revealed as one of the most prominent nodes in the TF
700 network (Fig. 6 and Fig. S5AT), but has not yet been characterized in *P. anserina*. *Pa_7_7000*

701 has orthologs in the seven species of the *Podospora* complex (Boucher, Nguyen, and Silar
702 2017) and in some fungi closely related to this species complex (*Cercophora samala*,
703 *Triangularia verruculosa* and *Apiosordaria backusii*). However, more distantly related species
704 (*Podospora setosa*, *Podospora australis*, *Podospora appendiculata*, *Thermothelomyces*
705 *thermophilus*, *Neurospora tetrasperma* and *Neurospora discreta*) contain a protein that shares
706 some identity with Pa_7_7000, but they all lack the Zn(II)2Cys6 domain and are therefore
707 unlikely to be functional orthologs. Wave V contains *Pa_6_11860*/*Fluffy* (Bailey and Ebbole
708 1998) (Fig. S5AT), which is required in *N. crassa* for the formation of conidia. These vegetative
709 spores are absent in *P. anserina*, suggesting that this gene has been recruited for ascospore
710 formation in this fungus, as in others members of the *P. anserina / P. pauciseta / P. comata*
711 species complex (Boucher, Nguyen, and Silar 2017).

712 **Comparison of mating-type target genes at different developmental stages**

713 A transcriptomic analysis of *P. anserina* was performed previously to determine the
714 FMR1 and FPR1 target genes required for fertilization (Bidard *et al*. 2011). The analysis
715 focused on the comparison of *mat*- and *mat*+ mycelia competent for fertilization, namely the
716 stage preceding the development of the perithecium. It was performed using the same methods
717 as described here. The analysis identified 69 genes upregulated in a *mat*- mycelium and 88
718 genes upregulated in a *mat*+ mycelium. Among these genes, we search for the DE genes
719 identified in this study. A total of 32 DE genes (46 %) were identified among the 69 genes
720 which were found to be upregulated in the *mat*- mycelium (Table S8) and 45 DE genes (51%)
721 are found among the *mat*+ upregulated genes (Table S9). A statistical analysis indicates that the
722 DE genes are over-represented in both categories, when compared with the 3,466 DE genes in
723 the 10,507 *P. anserina*'s gene models. This overrepresentation was higher for the *mat*+
724 upregulated genes (Chi^2, p-value = 0.0003) than for the *mat*- upregulated genes (Chi^2, p-value
725 = 0.0183). This result is likely due to the use of a *mat*+ maternal strain for the fruiting body
726 development presented here and indicates that half of the genes upregulated in fertilization
727 competent mycelium are also up-regulated in maternal tissues during perithecial development.
728

729 # Discussion

730 **Mating-type gene expression**

731 In this study, we analyzed on a genome-wide scale the transcriptional changes
732 associated with sexual development in *P. anserina* over a 10-time points course, from
733 fertilization to ascospore maturation. We found that more than 32% of the *P. anserina*'s genes
734 are differentially expressed during at least one interval covered by this kinetic. Interestingly,
735 more than 36% of the proteins encoded by these genes do not have a Pfam domain, suggesting
736 that a significant proportion of them remain functionally uncharacterized. Overall, the data
737 generated by our study are rich in novel players involved in fungal sexual reproduction and are
738 likely to provide an exploratory framework to analyze the pathways that are required for the
739 differentiation of the 15 different tissues identified in a perithecium (Bistis, Perkins, and Read
740 2003).

741 Among these 15 tissues, the ascogenous hyphae plays a central role in the sexual cycle,
742 since it is where karyogamy, meiosis and ascospore formation take place. Its formation starts
743 at T24 (Fig. 1) and requires the expression of the four mating-type genes: *FMR1*, *SMR1*, *SMR2*
744 and *FPR1* (Zickler *et al*. 1995; Arnaise *et al*. 2001). The ratio of ascogenous tissue to the other
745 tissues of the perithecium is low, potentially masking the zygotic expression profile. This
746 detection limit of our experiments can be assessed by searching the transcripts of *FMR1*, *SMR1*
747 and *SMR2*. These three mating-type genes are specific to the *mat-* nuclei, which come from the
748 male organs and are present only in the ascogonial cell and in the ascogenous hyphae. These
749 three mating-type genes are listed in the DE genes (Table S1), indicating unambiguously that
750 transcripts specific to the ascogenous hyphae are detected in our experiments, in spite of its
751 scarcity. Moreover, upregulations of *FMR1* and *SMR2* transcripts are detected as soon as T24,
752 correlating with the initial development of ascogenous hyphae (Table S1). In addition, 11 genes
753 upregulated in *mat-* fertilization competent mycelium are among the DE genes (Table S8),
754 confirming the detection of transcript from *mat-* male nuclei in the female organ. However, no
755 significant upregulation of the *mat-* mating-type transcripts is detected in the early steps of
756 perithecial development, *i.e.* from T0 to the formation of the ascogonial cell at T18 (Fig. 1).
757 Correspondingly, no wave I DE genes are identified in genes that accumulate transcripts in the
758 *mat-* mycelium (Table S8). The earliest DE genes upregulated in *mat-* competent mycelium
759 belong to wave II (n = 4). Wave IV, which corresponds to upregulation of *mat-* mating-type
760 genes and their correlated genes (Fig. 6), includes 412 genes (Fig. 3), among which six belong
761 to genes upregulated in *mat-* mycelium (Table S8). Overall, these data suggests that critical

762 target genes required for the development from fertilization to the formation of ascogonial cells
763 are not included in the DE genes, because their expression level is below the detection threshold
764 of microarrays. In contrast, the expression of genes required for the subsequent developmental
765 stages (differentiation of ascogenous hyphae, meiosis and ascospore formation) are indeed
766 detected in our experiments.

767 Surprisingly, *FPR1*/*Pa_1_20590*, the *mat+* specific mating type gene, does not belong
768 to the DE genes, although this gene is also required for the formation of ascogenous hyphae
769 (Zickler *et al*. 1995; Arnaise *et al*. 2001). It is likely that any changes in expression of this gene
770 in zygotic tissues is hidden by its transcription in the maternal tissues, which are predominant
771 in the fruiting body. We have however found 45 DE genes that are specifically upregulated in
772 *mat+* mycelium competent for fertilization (Table S9). Among these DE genes, 32 are direct or
773 indirect target genes of FPR1 (Bidard *et al*. 2011). Their detection proved that FPR1 target
774 genes do not escape our method, although FPR1 itself is not present in DE genes. Moreover,
775 detection starts in the early stages of perithecium development as suggested by FPR1 target
776 genes belonging to wave II (n = 9). Later stages are represented by FPR1 target genes belonging
777 to wave IV (n = 3) and V (n = 2). However, our experiments do not allow us to determine
778 unambiguously whether the differential expression of a gene occurs in the maternal or in the
779 zygotic tissues.

780 The analysis presented above indicates that our data are pertinent to reveal new
781 pathways in the development of meiotic tissues of P. anserina. Fertilization, which initiates the
782 development of meiotic tissues, is the best-known step of this process. Its molecular description
783 has beneficiated from the yeast model and has revealed that pheromone/pheromone receptor
784 interactions and downstream cascade signal were both conserved in Pezizomycotina and
785 Saccharomycotina (Wilson *et al*. 2021). Subsequent steps have been cytologically well
786 described in numerous fungi and appear specific to Pezizomycotina. In contrast to fertilization,
787 the molecular mechanisms underlying these various cell programmes are unknown. These blind
788 spots may be exemplified by two steps, which are critical in Pezizomycotina to produce
789 numerous genetically different asci from a single fertilization event : i) several models were
790 proposed for the internuclear recognition following mitotic divisions after fertilization, but no
791 one brings a decisive understanding of this phenomenon (Turgeon and Debuchy 2007), ii)
792 internuclear recognition is followed by the formation of dikaryotic cells and croziers, but the
793 molecular mechanisms controlling their formation are unknown. The similarity of dikaryotic
794 cells and croziers to the basidiomycete clamp cells, which require homeodomain transcription
795 factors for their formation, might suggest similar underlying regulatory circuits, but any

796 functions of homeoboxes in dikaryotic cell and crozier formation were dismissed (Coppin *et al*.
797 2012). A third instance of blind spot is the differentiation of croziers into meiocytes. Although
798 the role of peroxisomes in this event is well documented, the signal triggering the change in
799 cellular programme is unknown (Peraza Reyes and Berteaux-Lecellier 2013). Our analyses
800 revealed co-expression networks, which provide candidates for regulatory circuits of
801 perithecium development and may be involved in the processes presented above. Some
802 particular pathways are discussed below.

803 **Secondary metabolite gene are actively regulated during sexual development.**

804 As in *N. crassa* (Wang *et al*. 2022), *C. globosum* (Wang *et al*. 2019) and *A. nidulans*
805 (Liu *et al*. 2021), our results further support the active role of SMs in fungal sexual reproduction.
806 The evolutionary conservation of their expression profile, *i.e*. downregulation from fertilization
807 to meiosis followed by a coordinated upregulation during ascospore formation and maturation
808 suggests that SMs protect fungal progeny, *i.e*. ascospores, from animal predation. However, we
809 identified several genes of unknown function that were overexpressed during early phases. It is
810 therefore possible that these metabolites protect newly-formed fructification but also that they
811 are recruited to mediate developmental processes. This is reminiscent of the *Pa_5_2090/pks-6*
812 gene, which encodes the insecticidal polyketide neurosporin A produced at a similar
813 developmental stage by *S. macrospora* (Nowrousian 2009) and *N. crassa* (Zhao *et al*. 2017) to
814 protect fructifications from arthropod attack. Whether this gene product is also involved in the
815 process of morphogenesis is still an open question (Wang *et al*. 2022).

816 Our data reveals a relationship between sterigmatocystin synthesis and mating-type
817 genes by correlating expression of *PaAflR/Pa_2_7360*, *HMG5/Pa_1_13940* and
818 *HMG8/Pa_6_4110* (Table 6 and Fig. 6). PaAflR/Pa_2_7360 is a regulator of the
819 sterigmatocystin synthesis cluster (Shen *et al*. 2019), while HMG5/Pa_1_13940 and
820 HMG8/Pa_6_4110 are HMG-domain TFs acting as hubs of regulation for the mating-type
821 genes and mating-type target genes (Ait Benkhali *et al*. 2013; Gautier *et al*. 2018). Our results
822 suggest that PaAflR/Pa_2_7360 controls positively the transcription of the two other genes.
823 Over expression of PaAflR/Pa_2_7360 results in sterility, as does the over-expression of
824 HMG5/Pa_1_13940 (Shen *et al*. 2019; Ait Benkhali *et al*. 2013). This result is in agreement
825 with the positive transcriptional control of *HMG5/Pa_1_13940* by PaAflR/Pa_2_7360. To date,
826 *PaAflR/Pa_2_7360* has not been deleted in *P. anserina*, and although its orthologue in *A.*
827 *nidulans* has been knocked out, the effect on the sexual cycle remains poorly understood (Wang
828 *et al*. 2022).

829 **Het genes operates important but yet unknown roles in sexual reproduction**

830 This study unveiled an interesting regulation of the *het* genes, which are involved in
831 allorecognition and thus control the viability of heterokaryons formed after hyphal fusion
832 during vegetative growth (Daskalov 2023). However, heterokaryotic syncytia are not restricted
833 to vegetative thalli, as fertilization also leads to the formation of such multinucleate cells, and
834 accordingly, several *het* loci have been shown to control hybrid fertility in *P. anserina* (Ament-
835 Velásquez *et al*. 2020). When we compared the *het* genes expression profiles during sexual
836 reproduction with those assayed during IR (Bidard, Clavé, and Saupe 2013) and bacterial
837 defense response (Lamacchia *et al*. 2016) (Table S6 G), we found that they fall into two
838 categories and four classes.
839 The first category consists of het genes that were always down-regulated during sexual
840 reproduction but were either up-regulated during IR and/or bacterial confrontation (class 1) or
841 down-regulated during IR and up-regulated during bacterial confrontation (class 4). This
842 category therefore contains *het* genes that play a role only in vegetative growth and/or defense
843 against pathogens, but must otherwise be silenced.
844 The second category consisted of *het* genes that were either up-regulated during IR but
845 also at some time points during sexual reproduction (class 2) or were not DE during IR and
846 bacterial confrontation but during sexual reproduction (class 3). Class 2 genes may be recruited
847 to control cell fusion during morphogenesis of fructifications and/or of early zygotic lineage for
848 wave II genes, or of the developing asci and ascospores for waves IV and V genes. Class 3
849 genes may have been recruited to carry out specific programmed cell death events, not related
850 to hyphal fusion but necessary for sexual morphogenesis. In this context, *Pa_3_5550* is of
851 particular interest since it shows a peak of expression during dikaryon formation. Hce2 proteins
852 also belong to this category, suggesting a specific role during both the pre-zygotic (*Pa_2_4765*)
853 and post-zygotic (*Pa_1_17065*) stages.
854 The *het-6* and *het-13* genes were found to be DE during sexual reproduction in the
855 heterothallic fungus *N. crassa*, whereas no such observation was made in the homothallic
856 fungus *C. globosum* (Wang *et al*. 2019). In *P. anserina*, both orthologs *Pa_6_6160/het-6* and
857 *Pa_0_150/het-13* were also DE but showed opposite expression patterns compared to *N. crassa*.
858 This suggests that the roles of *het* genes, although central in the sexual developmental network
859 of fungi endowed with two different mating types, are polymorphic.
860 **Rewiring genes in the RNAi pathway?**
861 In *P. anserina* (Grognet *et al*. 2019), as in *T. reesei* (Li, Chen, and Wang 2018) and *A.*
862 *immersus* (Malagnac *et al*. 1997), the *rid* (*RIP defective*) ortholog is required for proper sexual
863 reproduction, which is not the case in *N. crassa*. *Pa_1_19440*/*PaRid* showed a short peak of

expression at T12 (Fig. S5AI), which is consistent with its requirement for the individualization of the dikaryotic cells leading to meiocytes (Grognet *et al*. 2019). In contrast, *N. crassa rid* up-regulation started at dikaryon formation and increased continuously throughout the second half of sexual reproduction (Wang *et al*. 2014). Interestingly, the *N. crassa rid* expression pattern was similar to that of the *P. anserina* DNA methyltransferase encoding gene *PaDnmt5*, which is absent in *N. crassa*. These results were in agreement with our previous data (Grognet *et al*. 2019) and strengthened the body of evidence pointing to a role for DNA methylation during sexual development.

Although there is no experimental proof that either somatic or meiotic RNAi pathways (Quelling or MSUD, respectively) works efficiently in *P. anserina*, some of the corresponding genes are found to be DE during sexual reproduction. Globally the expression patterns of *P. anserina* genes involved in the RNAi pathways are opposite to those of *N. crassa*, except for *Pa_2_9830/Sad-2* and *Pa_5_11380/Sad-5*. During MSUD, Sad-2 is thought to interact with the RdRP Sad-1 as a scaffold. Yet, *Sad-1* and *Sad-2* showed opposite patterns of expression during *N. crassa* sexual development, which likely discards this hypothesis (Wang *et al*. 2014). However, *Sad-5*, which role is yet unknown, has an expression profile that is similar to that of *Sad-2*. The evolutive conservation of *Pa_2_9830/Sad-2* and *Pa_5_11380/Sad-5* profiles of expression in both *N. crassa* and *P. anserina*, suggests that they have been recruited together to play a role in sexual reproduction. In the homothallic ascomycete *S. macrospora*, *Dcl1*, *Dcl2*, *Sms2* and *Qde2* are involved in meiocyte formation (Girard *et al*. 2021), which is not consistent with the expression pattern of the *Pa_6_6150/Dcl-1* but rather with that of *Pa_5_8910/Sms-2*. Altogether, these results suggest a complex role for the RNAi machinery during fungal sexual reproduction.

Conclusion

Our work reveals 3,466 DE genes during the differentiation of fruiting bodies of *P. anserina*. Only 86 of these DE genes have been previously functionally analyzed (Table S10), leaving a large number of genes for future investigations. Although our analysis does not allow us to determine the DE genes specifically expressed in each tissue of the fruiting body, our method is sensitive enough to detect DE genes in ascogenous hyphae, at a stage where this tissue is represented by few cells in the mass of the fruiting body. The sensitivity of our method is emphasized by the detection of a peak of transcription of *Pa_1_19440*/*PaRid* at a time of the early perithecial development corresponding to its expected function. Among the DE genes, we have identified at least two pathways that may control mating-type genes. The first one involves *Pa_7_7000*, possibly revealing a new regulatory pathway upstream of mating-type genes. The second one is the relationship between *PaAflR*/*Pa_2_7360*, *HMG5*/*Pa_1_13940* and *HMG8*/*Pa_6_4110*. The latter two TFs control mating-type genes, thus revealing an additional putative pathway regulating indirectly these genes. Our analysis reveals also the intriguing expression patterns of the genes from the MSUD and RNAi pathways, although MSUD has not been found in *P. anserina* and RNAi not investigated. Further research should be focused in *P. anserina* on the role of the genes involved in these pathways in other species.

Acknowledgements

We are grateful to S. Saupe for the exchange of data and ideas.

Funding

This work and the salary of F. Bidard were funded by the French National Research Agency (L'Agence Nationale de la Recherche, ANR) grant number ANR-05-BLAN-0385, project SexDevMycol, coordinator R. Debuchy.

Conflict of interest disclosure

The authors declare that they comply with the PCI rule of having no financial conflicts of interest in relation to the content of the article.

Data, scripts, code, and supplementary information availability

Data are available online: Go to https://www.ncbi.nlm.nih.gov/geo/query/acc.cgi?acc=GSE93094. Enter token whcrwemexfkfhqr into the box.

References

Ait Benkhali, Jinane, Evelyne Coppin, Sylvain Brun, Leonardo Peraza-Reyes, Tom Martin, Christina Dixelius, Noureddine Lazar, Herman van Tilbeurgh, and Robert Debuchy. 2013. 'A Network of HMG-Box Transcription Factors Regulates Sexual Cycle in the Fungus *Podospora anserina*'. *PLoS Genetics* 9 (7): e1003642. https://doi.org/10.1371/journal.pgen.1003642.

Ament-Velásquez, S. Lorena, Hanna Johannesson, Tatiana Giraud, Robert Debuchy, Sven J. Saupe, Alfons J.M. Debets, Eric Bastiaans, et al. 2020. 'The Taxonomy of the Model Filamentous Fungus *Podospora anserina*'. *MycoKeys* 75 (November):51–69. https://doi.org/10.3897/mycokeys.75.55968.

Arnaise, S., R. Debuchy, and M. Picard. 1997. 'What Is a Bona Fide Mating-Type Gene? Internuclear Complementation of Mat Mutants in *Podospora anserina*'. *Molecular & General Genetics: MGG* 256 (2): 169–78.

Arnaise, S., D. Zickler, S. Le Bilcot, C. Poisier, and R. Debuchy. 2001. 'Mutations in Mating-Type Genes of the Heterothallic Fungus *Podospora anserina* Lead to Self-Fertility'. *Genetics* 159 (2): 545–56.

Arnaise, Sylvie, Evelyne Coppin, Robert Debuchy, Denise Zickler, and Marguerite Picard. 1995. 'Models for Mating Type Gene Functions in *Podospora anserina*'. *Fungal Genetics Newsletter*, 42:79.

Ashburner, Michael, Catherine A. Ball, Judith A. Blake, David Botstein, Heather Butler, J. Michael Cherry, Allan P. Davis, et al. 2000. 'Gene Ontology: Tool for the Unification of Biology'. *Nature Genetics* 25 (1): 25–29. https://doi.org/10.1038/75556.

Bailey, Lori A, and Daniel J Ebbole. 1998. 'The Fluffy Gene of *Neurospora crassa* Encodes a Gal4p-Type C6 Zinc Cluster Protein Required for Conidial Development'. *Genetics* 148 (4): 1813–20. https://doi.org/10.1093/genetics/148.4.1813.

Basenko, Evelina Y., Jane A. Pulman, Achchuthan Shanmugasundram, Omar S. Harb, Kathryn Crouch, David Starns, Susanne Warrenfeltz, et al. 2018. 'FungiDB: An Integrated Bioinformatic Resource for Fungi and Oomycetes'. *Journal of Fungi* 4 (1): 39. https://doi.org/10.3390/jof4010039.

Bhetariya, Preetida J., Taruna Madan, Seemi Farhat Basir, Anupam Varma, and Sarma P. Usha. 2011. 'Allergens/Antigens, Toxins and Polyketides of Important Aspergillus Species'. *Indian Journal of Clinical Biochemistry* 26 (2): 104–19. https://doi.org/10.1007/s12291-011-0131-5.

Bian, K, Sap Lenz, Q Tang, F Chen, R Qi, M Jost, Cl Drennan, Jm Essigmann, Sd Wetmore, and D Li. 2019. 'DNA Repair Enzymes ALKBH2, ALKBH3, and AlkB Oxidize 5-Methylcytosine to 5-Hydroxymethylcytosine, 5-Formylcytosine and 5-Carboxylcytosine in Vitro'. *Nucleic Acids Research* 47 (11). https://doi.org/10.1093/nar/gkz395.

Bidard, F, S Imbeaud, N Reymond, O Lespinet, P Silar, C Clave, H Delacroix, V Berteaux-Lecellier, and R Debuchy. 2010. 'A General Framework for Optimization of Probes for Gene Expression Microarray and Its Application to the Fungus *Podospora anserina*' 3 (1): 171.

Bidard, Frédérique, Jinane Aït Benkhali, Evelyne Coppin, Sandrine Imbeaud, Pierre Grognet, Hervé Delacroix, and Robert Debuchy. 2011. 'Genome-Wide Gene Expression Profiling of Fertilization Competent Mycelium in Opposite Mating Types in the Heterothallic Fungus *Podospora anserina*'. *PloS One* 6 (6): e21476. https://doi.org/10.1371/journal.pone.0021476.

967 Bidard, Frédérique, Corinne Clavé, and Sven J. Saupe. 2013. 'The Transcriptional Response
968 to Nonself in the Fungus *Podospora anserina*'. *G3 (Bethesda, Md.)* 3 (6): 1015–30.
969 https://doi.org/10.1534/g3.113.006262.
970 Bistis, George, David Perkins, and Nick Read. 2003. 'Different Cell Types in *Neurospora*
971 *crassa*'. *Fungal Genetics Reports* 50 (1): 17–19. https://doi.org/10.4148/1941-
972 4765.1154.
973 Blank-Landeshammer, b, I Teichert, R Märker, M Nowrousian, U Kück, and A Sickmann.
974 2019. 'Combination of Proteogenomics with Peptide De Novo Sequencing Identifies
975 New Genes and Hidden Posttranscriptional Modifications'. *mBio* 10 (5).
976 https://doi.org/10.1128/mBio.02367-19.
977 Boisnard, Stéphanie, Eric Espagne, Denise Zickler, Anne Bourdais, Anne-Laure Riquet, and
978 Véronique Berteaux-Lecellier. 2009. 'Peroxisomal ABC Transporters and Beta-
979 Oxidation during the Life Cycle of the Filamentous Fungus *Podospora anserina*'.
980 *Fungal Genetics and Biology: FG & B* 46 (1): 55–66.
981 https://doi.org/10.1016/j.fgb.2008.10.006.
982 Bonnet, Crystel, Eric Espagne, Denise Zickler, Stéphanie Boisnard, Anne Bourdais, and
983 Véronique Berteaux-Lecellier. 2006. 'The Peroxisomal Import Proteins PEX2, PEX5
984 and PEX7 Are Differently Involved in *Podospora anserina* Sexual Cycle'. *Molecular*
985 *Microbiology* 62 (1): 157–69. https://doi.org/10.1111/j.1365-2958.2006.05353.x.
986 Borkovich, Katherine A., Lisa A. Alex, Oded Yarden, Michael Freitag, Gloria E. Turner,
987 Nick D. Read, Stephan Seiler, et al. 2004. 'Lessons from the Genome Sequence of
988 *Neurospora crassa*: Tracing the Path from Genomic Blueprint to Multicellular
989 Organism'. *Microbiology and Molecular Biology Reviews* 68 (1): 1–108.
990 https://doi.org/10.1128/mmbr.68.1.1-108.2004.
991 Boucher, Charlie, Tinh-Suong Nguyen, and Philippe Silar. 2017. 'Species Delimitation in the
992 *Podospora anserina*/*P. Pauciseta*/*P. Comata* Species Complex (Sordariales)'.
993 *Cryptogamie, Mycologie* 38 (4): 485–506.
994 Bouhouche, K, D Zickler, R Debuchy, and S Arnaise. 2004. 'Altering a Gene Involved in
995 Nuclear Distribution Increases the Repeat-Induced Point Mutation Process in the
996 Fungus *Podospora anserina*'. *Genetics* 167 (1): 151–59.
997 Boyle, Elizabeth I., Shuai Weng, Jeremy Gollub, Heng Jin, David Botstein, J. Michael
998 Cherry, and Gavin Sherlock. 2004. 'GO::TermFinder--Open Source Software for
999 Accessing Gene Ontology Information and Finding Significantly Enriched Gene
1000 Ontology Terms Associated with a List of Genes'. *Bioinformatics (Oxford, England)*
1001 20 (18): 3710–15. https://doi.org/10.1093/bioinformatics/bth456.
1002 Breyer, Eva, and Federico Baltar. 2023. 'The Largely Neglected Ecological Role of Oceanic
1003 Pelagic Fungi'. *Trends in Ecology & Evolution* 38 (9): 870–88.
1004 https://doi.org/10.1016/j.tree.2023.05.002.
1005 Carlier, F., M. Li, L. Maroc, R. Debuchy, C. Souaid, D. Noordermeer, P. Grognet, and F.
1006 Malagnac. 2021. 'Loss of EZH2-like or SU(VAR)3-9-like Proteins Causes
1007 Simultaneous Perturbations in H3K27 and H3K9 Tri-Methylation and Associated
1008 Developmental Defects in the Fungus *Podospora anserina*'. *Epigenetics & Chromatin*
1009 14 (1): 22. https://doi.org/10.1186/s13072-021-00395-7.
1010 Cheng, Steven Yan, and J. Michael Bishop. 2002. 'Suppressor of Fused Represses Gli-
1011 Mediated Transcription by Recruiting the SAP18-mSin3 Corepressor Complex'.
1012 *Proceedings of the National Academy of Sciences* 99 (8): 5442–47.
1013 https://doi.org/10.1073/pnas.082096999.
1014 Chevanne, Damien, Sven J Saupe, Corinne Clavé, and Mathieu Paoletti. 2010. 'WD-Repeat
1015 Instability and Diversification of the *Podospora anserina* Hnwd Non-Self Recognition

1016 Gene Family'. *BMC Evolutionary Biology* 10 (May):134.
1017 https://doi.org/10.1186/1471-2148-10-134.
1018 Cogoni, C, and G Macino. 1999. 'Gene Silencing in *Neurospora crassa* Requires a Protein
1019 Homologous to RNA-Dependent RNA Polymerase'. *Nature* 399 (6732): 166–69.
1020 https://doi.org/10.1038/20215.
1021 Coppin, E, and P Silar. 2007. 'Identification of PaPKS1, a Polyketide Synthase Involved in
1022 Melanin Formation and Its Use as a Genetic Tool in *Podospora anserina*'.
1023 *Mycological Research* 111 (Pt 8): 901–8.
1024 https://doi.org/10.1016/j.mycres.2007.05.011.
1025 Coppin, Evelyne, Véronique Berteaux-Lecellier, Frédérique Bidard, Sylvain Brun, Gwenaël
1026 Ruprich-Robert, Eric Espagne, Jinane Aït-Benkhali, et al. 2012. 'Systematic Deletion
1027 of Homeobox Genes in *Podospora anserina* Uncovers Their Roles in Shaping the
1028 Fruiting Body'. *PloS One* 7 (5): e37488.
1029 https://doi.org/10.1371/journal.pone.0037488.
1030 Cottingham, F. R., L. Gheber, D. L. Miller, and M. A. Hoyt. 1999. 'Novel Roles for
1031 *Saccharomyces cerevisiae* Mitotic Spindle Motors'. *The Journal of Cell Biology* 147
1032 (2): 335–50. https://doi.org/10.1083/jcb.147.2.335.
1033 Curto, M.-Ángeles, Mohammad Reza Sharifmoghadam, Eduardo Calpena, Nagore De León,
1034 Marta Hoya, Cristina Doncel, Janet Leatherwood, and M.-Henar Valdivieso. 2014.
1035 'Membrane Organization and Cell Fusion during Mating in Fission Yeast Requires
1036 Multipass Membrane Protein Prm1'. *Genetics* 196 (4): 1059–76.
1037 https://doi.org/10.1534/genetics.113.159558.
1038 Daskalov, Asen. 2023. 'Emergence of the Fungal Immune System'. *iScience* 26 (6): 106793.
1039 https://doi.org/10.1016/j.isci.2023.106793.
1040 Dyer, Paul S., and Ulrich Kück. 2017. 'Sex and the Imperfect Fungi'. *Microbiology Spectrum*
1041 5 (3): 10.1128/microbiolspec.funk-0043–2017.
1042 https://doi.org/10.1128/microbiolspec.funk-0043-2017.
1043 Edgar, Ron, Michael Domrachev, and Alex E. Lash. 2002. 'Gene Expression Omnibus: NCBI
1044 Gene Expression and Hybridization Array Data Repository'. *Nucleic Acids Research*
1045 30 (1): 207–10. https://doi.org/10.1093/nar/30.1.207.
1046 Emms, David M., and Steven Kelly. 2019. 'OrthoFinder: Phylogenetic Orthology Inference
1047 for Comparative Genomics'. *Genome Biology* 20 (1): 238.
1048 https://doi.org/10.1186/s13059-019-1832-y.
1049 Erdman, S., L. Lin, M. Malczynski, and M. Snyder. 1998. 'Pheromone-Regulated Genes
1050 Required for Yeast Mating Differentiation'. *The Journal of Cell Biology* 140 (3): 461–
1051 83. https://doi.org/10.1083/jcb.140.3.461.
1052 Espagne, Eric, Pascale Balhadère, Marie-Louise Penin, Christian Barreau, and Béatrice
1053 Turcq. 2002. 'HET-E and HET-D Belong to a New Subfamily of WD40 Proteins
1054 Involved in Vegetative Incompatibility Specificity in the Fungus *Podospora*
1055 *anserina*.' *Genetics* 161 (1): 71–81.
1056 Espagne, Eric, Olivier Lespinet, Fabienne Malagnac, Corinne Da Silva, Olivier Jaillon, Betina
1057 M Porcel, Arnaud Couloux, et al. 2008. 'The Genome Sequence of the Model
1058 Ascomycete Fungus *Podospora anserina*'. *Genome Biology* 9 (5): R77.
1059 https://doi.org/10.1186/gb-2008-9-5-r77.
1060 Foster, Benjamin M., Paul Stolz, Christopher B. Mulholland, Alex Montoya, Holger Kramer,
1061 Sebastian Bultmann, and Till Bartke. 2018. 'Critical Role of the UBL Domain in
1062 Stimulating the E3 Ubiquitin Ligase Activity of UHRF1 toward Chromatin'.
1063 *Molecular Cell* 72 (4): 739-752.e9. https://doi.org/10.1016/j.molcel.2018.09.028.

1064 Froehlich, Allan C., Yi Liu, Jennifer J. Loros, and Jay C. Dunlap. 2002. 'White Collar-1, a
1065 Circadian Blue Light Photoreceptor, Binding to the Frequency Promoter'. *Science*
1066 *(New York, N.Y.)* 297 (5582): 815–19. https://doi.org/10.1126/science.1073681.
1067 Galagan, James E, Sarah E Calvo, Katherine A Borkovich, Eric U Selker, Nick D Read,
1068 David Jaffe, William FitzHugh, et al. 2003. 'The Genome Sequence of the
1069 Filamentous Fungus *Neurospora crassa*'. *Nature* 422 (6934): 859–68.
1070 https://doi.org/10.1038/nature01554.
1071 Gautier, Valérie, Laetitia Chan Ho Tong, Tinh-Suong Nguyen, Robert Debuchy, and Philippe
1072 Silar. 2018. 'PaPro1 and IDC4, Two Genes Controlling Stationary Phase, Sexual
1073 Development and Cell Degeneration in *Podospora anserina*'. *Journal of Fungi (Basel,*
1074 *Switzerland)* 4 (3): 85. https://doi.org/10.3390/jof4030085.
1075 Girard, Chloe, Karine Budin, Stéphanie Boisnard, Liangran Zhang, Robert Debuchy, Denise
1076 Zickler, and Eric Espagne. 2021. 'RNAi-Related Dicer and Argonaute Proteins Play
1077 Critical Roles for Meiocyte Formation, Chromosome-Axes Lengths and Crossover
1078 Patterning in the Fungus *Sordaria macrospora*'. *Frontiers in Cell and Developmental*
1079 *Biology* 9 (June). https://doi.org/10.3389/fcell.2021.684108.
1080 Grognet, Pierre, Hélène Timpano, Florian Carlier, Jinane Aït-Benkhali, Véronique Berteaux-
1081 Lecellier, Robert Debuchy, Frédérique Bidard, and Fabienne Malagnac. 2019. 'A
1082 RID-like Putative Cytosine Methyltransferase Homologue Controls Sexual
1083 Development in the Fungus *Podospora anserina*'. *PLoS Genetics* 15 (8): e1008086.
1084 https://doi.org/10.1371/journal.pgen.1008086.
1085 He, Qiyang, Ping Cheng, Yuhong Yang, Lixing Wang, Kevin H. Gardner, and Yi Liu. 2002.
1086 'White Collar-1, a DNA Binding Transcription Factor and a Light Sensor'. *Science*
1087 *(New York, N.Y.)* 297 (5582): 840–43. https://doi.org/10.1126/science.1072795.
1088 Hutchison, Elizabeth A, and N Louise Glass. 2010. 'Meiotic Regulators Ndt80 and Ime2
1089 Have Different Roles in Saccharomyces and Neurospora'. *Genetics* 185 (4): 1271–82.
1090 https://doi.org/10.1534/genetics.110.117184.
1091 Iliev, Iliyan D., Gordon D. Brown, Petra Bacher, Sarah L. Gaffen, Joseph Heitman, Bruce S.
1092 Klein, and Michail S. Lionakis. 2024. 'Focus on Fungi'. *Cell* 187 (19): 5121–27.
1093 https://doi.org/10.1016/j.cell.2024.08.016.
1094 Imbeaud, Sandrine, Esther Graudens, Virginie Boulanger, Xavier Barlet, Patrick Zaborski,
1095 Eric Eveno, Odilo Mueller, Andreas Schroeder, and Charles Auffray. 2005. 'Towards
1096 Standardization of RNA Quality Assessment Using User-Independent Classifiers of
1097 Microcapillary Electrophoresis Traces'. *Nucleic Acids Research* 33 (6): e56.
1098 https://doi.org/10.1093/nar/gni054.
1099 Julius, D., A. Brake, L. Blair, R. Kunisawa, and J. Thorner. 1984. 'Isolation of the Putative
1100 Structural Gene for the Lysine-Arginine-Cleaving Endopeptidase Required for
1101 Processing of Yeast Prepro-Alpha-Factor'. *Cell* 37 (3): 1075–89.
1102 https://doi.org/10.1016/0092-8674(84)90442-2.
1103 Kaneko, Isao, Karine Dementhon, Qijun Xiang, and N. Louise Glass. 2006. 'Nonallelic
1104 Interactions between Het-c and a Polymorphic Locus, Pin-c, Are Essential for Nonself
1105 Recognition and Programmed Cell Death in *Neurospora crassa*'. *Genetics* 172 (3):
1106 1545–55. https://doi.org/10.1534/genetics.105.051490.
1107 Kerr, M. K., and G. A. Churchill. 2001. 'Statistical Design and the Analysis of Gene
1108 Expression Microarray Data'. *Genetical Research* 77 (2): 123–28.
1109 https://doi.org/10.1017/s0016672301005055.
1110 Kim, Wonyong, Zheng Wang, Hyeonjae Kim, Kasey Pham, Yujia Tu, Jeffrey P. Townsend,
1111 and Frances Trail. 2022. 'Transcriptional Divergence Underpinning Sexual
1112 Development in the Fungal Class Sordariomycetes'. *mBio*, May, e0110022.
1113 https://doi.org/10.1128/mbio.01100-22.

1114 Kurahashi, Hiroshi, Yoshiyuki Imai, and Masayuki Yamamoto. 2002. 'Tropomyosin Is
1115 Required for the Cell Fusion Process during Conjugation in Fission Yeast'. *Genes to*
1116 *Cells: Devoted to Molecular & Cellular Mechanisms* 7 (4): 375–84.
1117 https://doi.org/10.1046/j.1365-2443.2002.00526.x.
1118 Lamacchia, Marina, Witold Dyrka, Annick Breton, Sven J. Saupe, and Mathieu Paoletti.
1119 2016. 'Overlapping *Podospora anserina* Transcriptional Responses to Bacterial and
1120 Fungal Non Self Indicate a Multilayered Innate Immune Response'. *Frontiers in*
1121 *Microbiology* 7:471. https://doi.org/10.3389/fmicb.2016.00471.
1122 Leipe, Detlef D., Eugene V. Koonin, and L. Aravind. 2004. 'STAND, a Class of P-Loop
1123 NTPases Including Animal and Plant Regulators of Programmed Cell Death: Multiple,
1124 Complex Domain Architectures, Unusual Phyletic Patterns, and Evolution by
1125 Horizontal Gene Transfer'. *Journal of Molecular Biology* 343 (1): 1–28.
1126 https://doi.org/10.1016/j.jmb.2004.08.023.
1127 Li, Wan-Chen, Chia-Ling Chen, and Ting-Fang Wang. 2018. 'Repeat-Induced Point (RIP)
1128 Mutation in the Industrial Workhorse Fungus *Trichoderma reesei*'. *Applied*
1129 *Microbiology and Biotechnology*, January. https://doi.org/10.1007/s00253-017-8731-
1130 5.
1131 Liu, Li, Christoph Sasse, Benedict Dirnberger, Oliver Valerius, Enikő Fekete-Szücs, Rebekka
1132 Harting, Daniela E Nordzieke, et al. 2021. 'Secondary Metabolites of Hülle Cells
1133 Mediate Protection of Fungal Reproductive and Overwintering Structures against
1134 Fungivorous Animals'. Edited by Antonis Rokas, Detlef Weigel, Milton Drott, and
1135 Jae-Hyuk Yu. *eLife* 10 (October):e68058. https://doi.org/10.7554/eLife.68058.
1136 Lütkenhaus, Ramona, Stefanie Traeger, Jan Breuer, Laia Carreté, Alan Kuo, Anna Lipzen,
1137 Jasmyn Pangilinan, et al. 2019. 'Comparative Genomics and Transcriptomics to
1138 Analyze Fruiting Body Development in Filamentous Ascomycetes'. *Genetics*,
1139 October. https://doi.org/10.1534/genetics.119.302749.
1140 MacPherson, Sarah, Marc Larochelle, and Bernard Turcotte. 2006. 'A Fungal Family of
1141 Transcriptional Regulators: The Zinc Cluster Proteins'. *Microbiology and Molecular*
1142 *Biology Reviews* 70 (3): 583–604. https://doi.org/10.1128/mmbr.00015-06.
1143 Malagnac, F, B Wendel, C Goyon, G Faugeron, D Zickler, J L Rossignol, M Noyer-Weidner,
1144 P Vollmayr, T A Trautner, and J Walter. 1997. 'A Gene Essential for de Novo
1145 Methylation and Development in Ascobolus Reveals a Novel Type of Eukaryotic
1146 DNA Methyltransferase Structure'. *Cell* 91 (2): 281–90.
1147 Mistry, Jaina, Sara Chuguransky, Lowri Williams, Matloob Qureshi, Gustavo A. Salazar, Erik
1148 L. L. Sonnhammer, Silvio C. E. Tosatto, et al. 2021. 'Pfam: The Protein Families
1149 Database in 2021'. *Nucleic Acids Research* 49 (D1): D412–19.
1150 https://doi.org/10.1093/nar/gkaa913.
1151 Nelson, M. A., S. T. Merino, and R. L. Metzenberg. 1997. 'A Putative Rhamnogalacturonase
1152 Required for Sexual Development of *Neurospora crassa*'. *Genetics* 146 (2): 531–40.
1153 https://doi.org/10.1093/genetics/146.2.531.
1154 Nowrousian, Minou. 2009. 'A Novel Polyketide Biosynthesis Gene Cluster Is Involved in
1155 Fruiting Body Morphogenesis in the Filamentous Fungi *Sordaria macrospora* and
1156 *Neurospora crassa*'. *Current Genetics* 55 (2): 185–98. https://doi.org/10.1007/s00294-
1157 009-0236-z.
1158 Nowrousian, Minou. 2022. 'The Role of Chromatin and Transcriptional Control in the
1159 Formation of Sexual Fruiting Bodies in Fungi'. *Microbiology and Molecular Biology*
1160 *Reviews: MMBR* 86 (4): e0010422. https://doi.org/10.1128/mmbr.00104-22.
1161 Oh, Yong-Seok, Pu Gao, Ko-Woon Lee, Ilaria Ceglia, Ji-Seon Seo, Xiaozhu Zhang, Jung-
1162 Hyuck Ahn, et al. 2013. 'SMARCA3, a Chromatin-Remodeling Factor, Is Required

1163 for P11-Dependent Antidepressant Action'. *Cell* 152 (4): 831–43.
1164 https://doi.org/10.1016/j.cell.2013.01.014.
1165 Ottmann, Christian, Borries Luberacki, Isabell Küfner, Wolfgang Koch, Frédéric Brunner,
1166 Michael Weyand, Laura Mattinen, et al. 2009. 'A Common Toxin Fold Mediates
1167 Microbial Attack and Plant Defense'. *Proceedings of the National Academy of*
1168 *Sciences* 106 (25): 10359–64. https://doi.org/10.1073/pnas.0902362106.
1169 Otto, Sarah P. 2009. 'The Evolutionary Enigma of Sex'. *The American Naturalist* 174 Suppl 1
1170 (July):S1–14. https://doi.org/10.1086/599084.
1171 Pearl, LH. 2000. 'Structure and Function in the Uracil-DNA Glycosylase Superfamily'.
1172 *Mutation Research* 460 (3–4). https://doi.org/10.1016/s0921-8777(00)00025-2.
1173 Peraza Reyes, Leonardo, and Véronique Berteaux-Lecellier. 2013. 'Peroxisomes and Sexual
1174 Development in Fungi'. *Frontiers in Physiology* 4.
1175 https://doi.org/10.3389/fphys.2013.00244.
1176 Peraza-Reyes, Leonardo, and Fabienne Malagnac. 2016. *Sexual Development in Fungi*. The
1177 Mycota I, Growth, Differentiation and Sexuality. Springer.
1178 Rizet, G, and C Engelmann. 1949. 'Contribution à l'étude Génétique d'un Ascomycète
1179 Tétrasporé: *Podospora anserina*' 11:201–304.
1180 Romano, Nicoletta, and Giuseppe Macino. 1992. 'Quelling: Transient Inactivation of Gene
1181 Expression in *Neurospora crassa* by Transformation with Homologous Sequences'.
1182 *Molecular Microbiology* 6 (22): 3343–53. https://doi.org/10.1111/j.1365-
1183 2958.1992.tb02202.x.
1184 Rose, M. D., L. M. Misra, and J. P. Vogel. 1989. 'KAR2, a Karyogamy Gene, Is the Yeast
1185 Homolog of the Mammalian BiP/GRP78 Gene'. *Cell* 57 (7): 1211–21.
1186 https://doi.org/10.1016/0092-8674(89)90058-5.
1187 Shen, Ling, François-Hugues Porée, Thomas Gaslonde, Hervé Lalucque, Florence Chapeland-
1188 Leclerc, and Gwenaël Ruprich-Robert. 2019. 'Functional Characterization of the
1189 Sterigmatocystin Secondary Metabolite Gene Cluster in the Filamentous Fungus
1190 *Podospora anserina*: Involvement in Oxidative Stress Response, Sexual Development,
1191 Pigmentation and Interspecific Competitions'. *Environmental Microbiology* 21 (8):
1192 3011–26. https://doi.org/10.1111/1462-2920.14698.
1193 Shiu, P K, N B Raju, D Zickler, and R L Metzenberg. 2001. 'Meiotic Silencing by Unpaired
1194 DNA'. *Cell* 107 (7): 905–16.
1195 Silar, Philippe. 2020. *Podospora anserina*. https://hal.archives-ouvertes.fr/hal-02475488.
1196 Slot, Jason C., and Antonis Rokas. 2011. 'Horizontal Transfer of a Large and Highly Toxic
1197 Secondary Metabolic Gene Cluster between Fungi'. *Current Biology: CB* 21 (2): 134–
1198 39. https://doi.org/10.1016/j.cub.2010.12.020.
1199 Stajich, Jason E., Mary L. Berbee, Meredith Blackwell, David S. Hibbett, Timothy Y. James,
1200 Joseph W. Spatafora, and John W. Taylor. 2009. 'The Fungi'. *Current Biology* 19
1201 (18): R840–45. https://doi.org/10.1016/j.cub.2009.07.004.
1202 Steffens, Eva Katharina, Kordula Becker, Sabine Krevet, Ines Teichert, and Ulrich Kück.
1203 2016. 'Transcription Factor PRO1 Targets Genes Encoding Conserved Components of
1204 Fungal Developmental Signaling Pathways'. *Molecular Microbiology* 102 (5): 792–
1205 809. https://doi.org/10.1111/mmi.13491.
1206 Stergiopoulos, Ioannis, Jérôme Collemare, Rahim Mehrabi, and Pierre J. G. M. De Wit. 2013.
1207 'Phytotoxic Secondary Metabolites and Peptides Produced by Plant Pathogenic
1208 Dothideomycete Fungi'. *FEMS Microbiology Reviews* 37 (1): 67–93.
1209 https://doi.org/10.1111/j.1574-6976.2012.00349.x.
1210 Sun, Xianyun, Luning Yu, Nan Lan, Shiping Wei, Yufei Yu, Hanxing Zhang, Xinyu Zhang,
1211 and Shaojie Li. 2012. 'Analysis of the Role of Transcription Factor VAD-5 in

1212 Conidiation of *Neurospora crassa*'. *Fungal Genetics and Biology* 49 (5): 379–87.
1213 https://doi.org/10.1016/j.fgb.2012.03.003.
1214 Teichert, Ines, Tim A. Dahlmann, Ulrich Kück, and Minou Nowrousian. 2017. 'RNA Editing
1215 During Sexual Development Occurs in Distantly Related Filamentous Ascomycetes'.
1216 *Genome Biology and Evolution* 9 (4): 855–68. https://doi.org/10.1093/gbe/evx052.
1217 Teichert, Ines, Stefanie Pöggeler, and Minou Nowrousian. 2020. '*Sordaria macrospora*:
1218 25 Years as a Model Organism for Studying the Molecular Mechanisms of Fruiting
1219 Body Development'. *Applied Microbiology and Biotechnology* 104 (9): 3691–3704.
1220 https://doi.org/10.1007/s00253-020-10504-3.
1221 Teichert, Ines, Gabriele Wolff, Ulrich Kück, and Minou Nowrousian. 2012. 'Combining
1222 Laser Microdissection and RNA-Seq to Chart the Transcriptional Landscape of Fungal
1223 Development'. *BMC Genomics* 13 (1): 511. https://doi.org/10.1186/1471-2164-13-
1224 511.
1225 The Gene Ontology Consortium, Suzi A Aleksander, James Balhoff, Seth Carbon, J Michael
1226 Cherry, Harold J Drabkin, Dustin Ebert, et al. 2023. 'The Gene Ontology
1227 Knowledgebase in 2023'. *Genetics* 224 (1): iyad031.
1228 https://doi.org/10.1093/genetics/iyad031.
1229 Thompson-Coffe, C., G. Borioli, D. Zickler, and A. L. Rosa. 1999. 'Pyruvate Decarboxylase
1230 Filaments Are Associated with the Cortical Cytoskeleton of Asci and Spores over the
1231 Sexual Cycle of Filamentous Ascomycetes'. *Fungal Genetics and Biology: FG & B* 26
1232 (1): 71–80. https://doi.org/10.1006/fgbi.1998.1106.
1233 Tong, Kevin, Thomas Keller, Charles S. Hoffman, and Anthony T. Annunziato. 2012.
1234 '*Schizosaccharomyces pombe* Hat1 (Kat1) Is Associated with Mis16 and Is Required
1235 for Telomeric Silencing'. *Eukaryotic Cell* 11 (9): 1095–1103.
1236 https://doi.org/10.1128/EC.00123-12.
1237 Turgeon, B Gillian, and R. Debuchy. 2007. 'Cochliobolus and Podospora: Mechanism of Sex
1238 Determination and the Evolution of Reproductive Lifestyle'. In *Sex in Fungi,*
1239 *Molecular Determination and Evolutionary Implications*.
1240 Wang, Amy, Siavash K. Kurdistani, and Michael Grunstein. 2002. 'Requirement of Hos2
1241 Histone Deacetylase for Gene Activity in Yeast'. *Science (New York, N.Y.)* 298
1242 (5597): 1412–14. https://doi.org/10.1126/science.1077790.
1243 Wang, Chengshu, and Raymond J. St Leger. 2007. 'The MAD1 Adhesin of Metarhizium
1244 Anisopliae Links Adhesion with Blastospore Production and Virulence to Insects, and
1245 the MAD2 Adhesin Enables Attachment to Plants'. *Eukaryotic Cell* 6 (5): 808–16.
1246 https://doi.org/10.1128/EC.00409-06.
1247 Wang, Peng, Jia Xu, Perng-Kuang Chang, Zhemin Liu, and Qing Kong. 2022. 'New Insights
1248 of Transcriptional Regulator AflR in *Aspergillus flavus* Physiology'. *Microbiology*
1249 *Spectrum* 10 (1): e00791-21. https://doi.org/10.1128/spectrum.00791-21.
1250 Wang, Zheng, Aditya Gudibanda, Ugochukwu Ugwuowo, Frances Trail, and Jeffrey P.
1251 Townsend. 2018. 'Using Evolutionary Genomics, Transcriptomics, and Systems
1252 Biology to Reveal Gene Networks Underlying Fungal Development'. *Fungal Biology*
1253 *Reviews*, Complex multicellularity in Fungi, 32 (4): 249–64.
1254 https://doi.org/10.1016/j.fbr.2018.02.001.
1255 Wang, Zheng, Francesc Lopez-Giraldez, Nina Lehr, Marta Farré, Ralph Common, Frances
1256 Trail, and Jeffrey P Townsend. 2014. 'Global Gene Expression and Focused Knockout
1257 Analysis Reveals Genes Associated with Fungal Fruiting Body Development in
1258 *Neurospora crassa*'. *Eukaryotic Cell* 13 (1): 154–69.
1259 https://doi.org/10.1128/EC.00248-13.
1260 Wang, Zheng, Francesc Lopez-Giraldez, Jason Slot, Oded Yarden, Frances Trail, and Jeffrey
1261 P. Townsend. 2022. 'Secondary Metabolism Gene Clusters Exhibit Increasingly

1262 Dynamic and Differential Expression during Asexual Growth, Conidiation, and Sexual
1263 Development in *Neurospora crassa*'. *mSystems* 7 (3): e00232-22.
1264 https://doi.org/10.1128/msystems.00232-22.
1265 Wang, Zheng, Francesc López-Giráldez, Junrui Wang, Frances Trail, and Jeffrey P.
1266 Townsend. 2019. 'Integrative Activity of Mating Loci, Environmentally Responsive
1267 Genes, and Secondary Metabolism Pathways during Sexual Development of
1268 *Chaetomium globosum*'. *mBio* 10 (6): 10.1128/mbio.02119-19.
1269 https://doi.org/10.1128/mbio.02119-19.
1270 White, B. T., and C. Yanofsky. 1993. 'Structural Characterization and Expression Analysis of
1271 the Neurospora Conidiation Gene Con-6'. *Developmental Biology* 160 (1): 254–64.
1272 https://doi.org/10.1006/dbio.1993.1303.
1273 Wilson, Andi M., P. Markus Wilken, Magriet A. van der Nest, Michael J. Wingfield, and
1274 Brenda D. Wingfield. 2019. 'It's All in the Genes: The Regulatory Pathways of Sexual
1275 Reproduction in Filamentous Ascomycetes'. *Genes* 10 (5): 330.
1276 https://doi.org/10.3390/genes10050330.
1277 Wilson, Andi M., P. Markus Wilken, Michael J. Wingfield, and Brenda D. Wingfield. 2021.
1278 'Genetic Networks That Govern Sexual Reproduction in the Pezizomycotina'.
1279 *Microbiology and Molecular Biology Reviews* 85 (4): e00020-21.
1280 https://doi.org/10.1128/MMBR.00020-21.
1281 Wolfe, Cecily J., Isaac S. Kohane, and Atul J. Butte. 2005. 'Systematic Survey Reveals
1282 General Applicability of "Guilt-by-Association" within Gene Coexpression
1283 Networks'. *BMC Bioinformatics* 6 (1): 227. https://doi.org/10.1186/1471-2105-6-227.
1284 Yang, Qiuying, Qiaohong Anne Ye, and Yi Liu. 2015. 'Mechanism of siRNA Production
1285 from Repetitive DNA'. *Genes & Development* 29 (5): 526–37.
1286 https://doi.org/10.1101/gad.255828.114.
1287 Young, B. P., R. A. Craven, P. J. Reid, M. Willer, and C. J. Stirling. 2001. 'Sec63p and Kar2p
1288 Are Required for the Translocation of SRP-Dependent Precursors into the Yeast
1289 Endoplasmic Reticulum in Vivo'. *The EMBO Journal* 20 (1–2): 262–71.
1290 https://doi.org/10.1093/emboj/20.1.262.
1291 Zhao, Yanxia, Jianing Ding, Weihua Yuan, Jinjin Huang, Wenxiu Huang, Yan Wang, and
1292 Weifa Zheng. 2017. 'Production of a Fungal Furocoumarin by a Polyketide Synthase
1293 Gene Cluster Confers the Chemo-Resistance of *Neurospora crassa* to the Predation by
1294 Fungivorous Arthropods'. *Environmental Microbiology* 19 (10): 3920–29.
1295 https://doi.org/10.1111/1462-2920.13791.
1296 Zheng, Qian, Rui Hou, null Juanyu, null Zhang, Jiwen Ma, Zhongshou Wu, Guanghui Wang,
1297 Chenfang Wang, and Jin-Rong Xu. 2013. 'The MAT Locus Genes Play Different
1298 Roles in Sexual Reproduction and Pathogenesis in *Fusarium graminearum*'. *PloS One*
1299 8 (6): e66980. https://doi.org/10.1371/journal.pone.0066980.
1300 Zickler, D., S. Arnaise, E. Coppin, R. Debuchy, and M. Picard. 1995. 'Altered Mating-Type
1301 Identity in the Fungus *Podospora anserina* Leads to Selfish Nuclei, Uniparental
1302 Progeny, and Haploid Meiosis'. *Genetics* 140 (2): 493–503.
1303